

CONTENTS

CHAPTER 6

THE GALACTIC PLANE

6.1 THE GALACTIC PLANE AT 2° RESOLUTION	
Absorption in the Galactic plane	6.1
The warp of the Galactic plane	6.3
6.2 GALACTIC PLANE AT THE FULL RESOLUTION	
Signal-to-noise ratio in the maps	6.4
The paucity of point sources towards the inner Galaxy	6.4
Discrete absorptions in the Galactic plane	6.5
6.3 DISCRETE ABSORPTIONS—A DISCUSSION	
Distances and the electron densities of the absorption features	6.6
Comparison with optical nebulosities	6.9
Galactic ridge recombination lines	6.13
Discrete absorptions seen at 34.5 MHz and their relation to GRRLs	6.14
What are the discrete absorptions ?	6.16
Conclusions	6.19
REFERENCES	6.21

Chapter 6

THE GALACTIC PLANE

In this chapter we shall discuss the galactic plane within $\pm 10^\circ$ of the galactic equator. Section 6.1 deals with some of the large scale features seen on the map smoothed to 2° resolution; we shall also make a comparison with the 408 MHz map. The galactic plane maps at the full resolution of $26' \times 33' \text{sec} (6 - 14.1)$ are presented in section 6.2. In Section 6.3 we shall make some detailed comments about the discrete absorptions seen at 34.5 MHz, their optical correspondences and their possible contribution to the galactic ridge recombination lines.

6.1 THE GALACTIC PLANE AT 2° RESOLUTION

The galactic plane from $l = 0^\circ$ to $l = 260^\circ$ and within $|b| < 20^\circ$ is shown in Fig. 6.1. In order to highlight the large angular scale structures we have smoothed our 34.5 MHz maps to 2° resolution. Figure 6.2 is the 408 MHz map at a similar resolution of the same region. The data for the 408 MHz map was obtained from the all-sky survey of Haslam et al. (1982). We indicate below some of the interesting features that we see in the 34.5 MHz map and the inferences one can draw when a comparison is made with the 408 MHz map.

6.1.1 Absorption in the Galactic plane

A comparison of the two maps shows that there is considerable absorption at 34.5 MHz in the inner Galaxy. Although for $|b| > 5^\circ$ the density of contours is about the same in both the maps, the ridge of emission, around $b = 0^\circ$ seen prominently in the

408 MHz map is absent at 34.5 MHz (This is an effect analogous to chopping off the top of the hill). No such effect is evident in the outer Galaxy.

This qualitative picture is quantified in the figures 6.3 and 6.4. Figure 6.3 shows the normalised brightness temperature at 408 MHz at $l = 10^\circ$ as a function of the galactic latitude (solid line). The crosses indicate the corresponding values at 34.5 MHz. Both profiles agree around $|b| \approx 20^\circ$ for a temperature spectral index between 408 MHz and 34.5 MHz, $\beta_{408}^{34.5} = -2.7$ (temperature \propto frequency $^\beta$). But for $|b| < 5^\circ$ it can be seen that there is considerable absorption at 34.5 MHz. Figure 6.4 shows a similar exercise done at $l = 180^\circ$. The value of $\beta_{408}^{34.5}$ used here to scale the 408 MHz temperatures is -2.55. It can be seen that in these directions there is no significant absorption at 34.5 MHz.

A more detailed picture is borne out by the temperature spectral index map obtained between 34.5 MHz and 408 MHz. In the longitude range $0^\circ < l < 30^\circ$, $\beta_{408}^{34.5} > -2.5$ for $|b| < 3^\circ$, and becomes steeper ($\beta_{408}^{34.5} = -2.7$) as one moves away from the plane. From $l = 30^\circ$ to $l = 50^\circ$, the width of the region of flatter temperature spectral index narrows down to $|b| < 1^\circ$. Beyond $l = 50^\circ$, no such effect is apparent - *i.e.* there is no systematic change in the temperature spectral index as a function of the Galactic latitude. Reich and Reich (1988) have obtained a temperature spectral index map of the Galaxy between 1420 MHz and 408 MHz. In the longitude range $0^\circ < l < 90^\circ$, the temperature spectral index, β_{1420}^{408} , is very close to -2.7 and does not have any systematic variation with the Galactic latitude. This **compared**

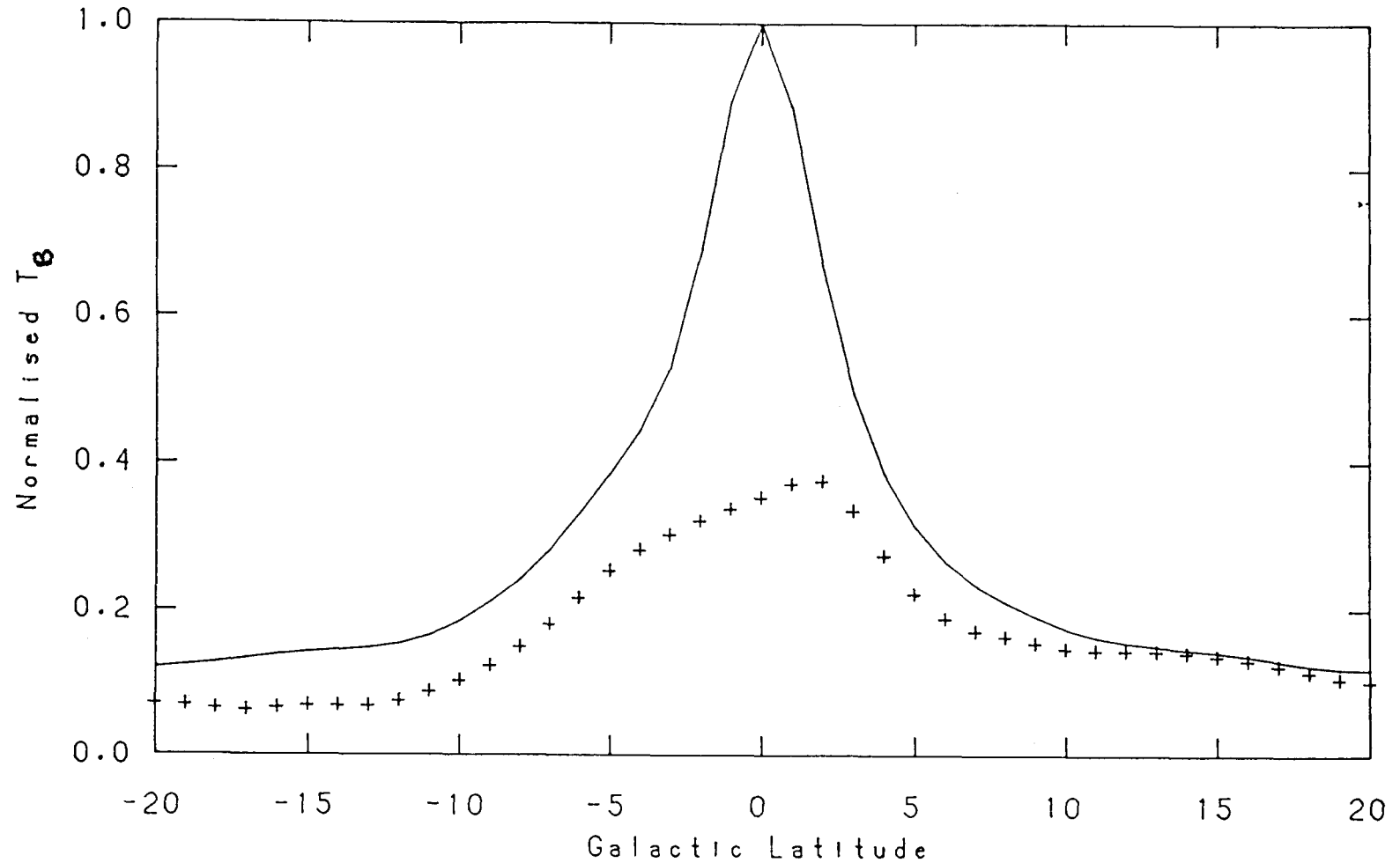
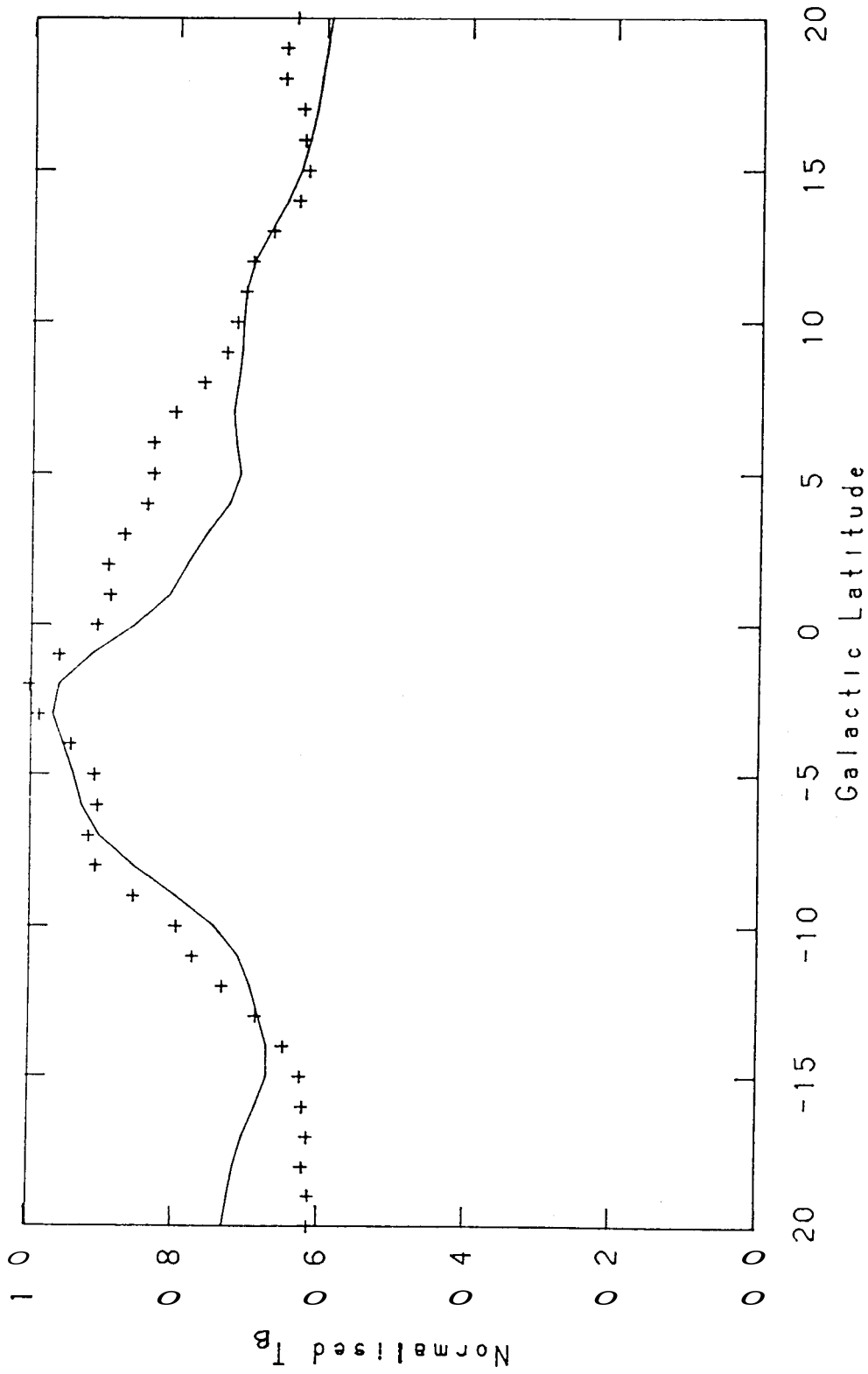


Fig. 6.3: Absorption of the galactic background at low frequencies in the inner Galaxy. The solid curve represents the normalised brightness temperature profile at 408 MHz obtained from the 2° convolved map. The crosses represent the brightness temperature profile at 34.5 MHz. Both the profiles roughly match around $|b| \approx 20^\circ$ with a temperature spectral index of -2.7 between 408 MHz and 34.5 MHz. Both the profiles were obtained at $l = 10^\circ$.



Fi 6.4: Profiles obtained from the 2° convolved maps at 408 MHz (solid line) and at 34.5 MHz (crosses) at a longitude of 180° . A temperature spectral index of -2.55 gives an overall agreement.

with our results is indicative of absorption at low frequencies in the plane of the Galaxy.

Towards the Galactic anticentre direction, $\beta_{1420}^{408} = -2.7$ but $\beta_{408}^{34.5} = -2.5$. However, in this direction there is no systematic latitude variation of $\beta_{408}^{34.5}$ and hence seems difficult to interpret the flatter spectral index at lower frequencies as due to absorption. One is thus forced to interpret this in terms of a break in the spectrum of the background radiation in the anticentre direction.

6.1.2 The Warp of the Galactic plane

Figure 6.1 also shows that the 'plane of the Galaxy' as defined by the centroid of emission does not always lie at $b = 0^\circ$, but wanders. Between $l = 75^\circ$ and $l = 90^\circ$, the centroid deviates from $b = 0^\circ$ by as much as $+5^\circ$. Between $l = 165^\circ$ and $l = 195^\circ$, the galactic plane is again not coincident with $b = 0^\circ$; here the centroid shifts to $b = -5^\circ$. This 'warp' can also be seen clearly in the 408 MHz map shown in Fig. 6.2 (Salter C.J.; personal communication). Since most of the emission in these longitude ranges is presumably from the External (Perseus) arm, it is tempting to suggest that perhaps the External arm is tilted with respect to the rest of the disc of the Galaxy. The warping of the disk of our own Galaxy and of external galaxies is also well known from neutral hydrogen observations (Kerr 1957; Sancisi 1976). Further studies correlating both the neutral hydrogen distribution and the non-thermal emission should throw more light on the nature of the warp.

6.2 GALACTIC PLANE AT THE FULL RESOLUTION

This section contains maps of the Galactic plane ($\pm 10^\circ$) at the full resolution of **GEETEE**. Alongside each 34.5 MHz map, the corresponding 408 MHz map is also given for easy comparison. Contour levels and labelling are as explained in chapter 4. The part of the galactic plane lying between $l = 105^\circ$ and $l = 135^\circ$ is not included since the presence of the residual sidelobes of Cas A in that region have rendered the map unusable.

The resolution of the 34.5 MHz maps is $21' \times 33''_{\text{sec}} (6 - 14.1)$ and the point sources display this elliptic beam. In addition, as one moves along the plane, the orientation of the beam changes as expected. The 408 MHz maps have a resolution of $51' \times 51'$.

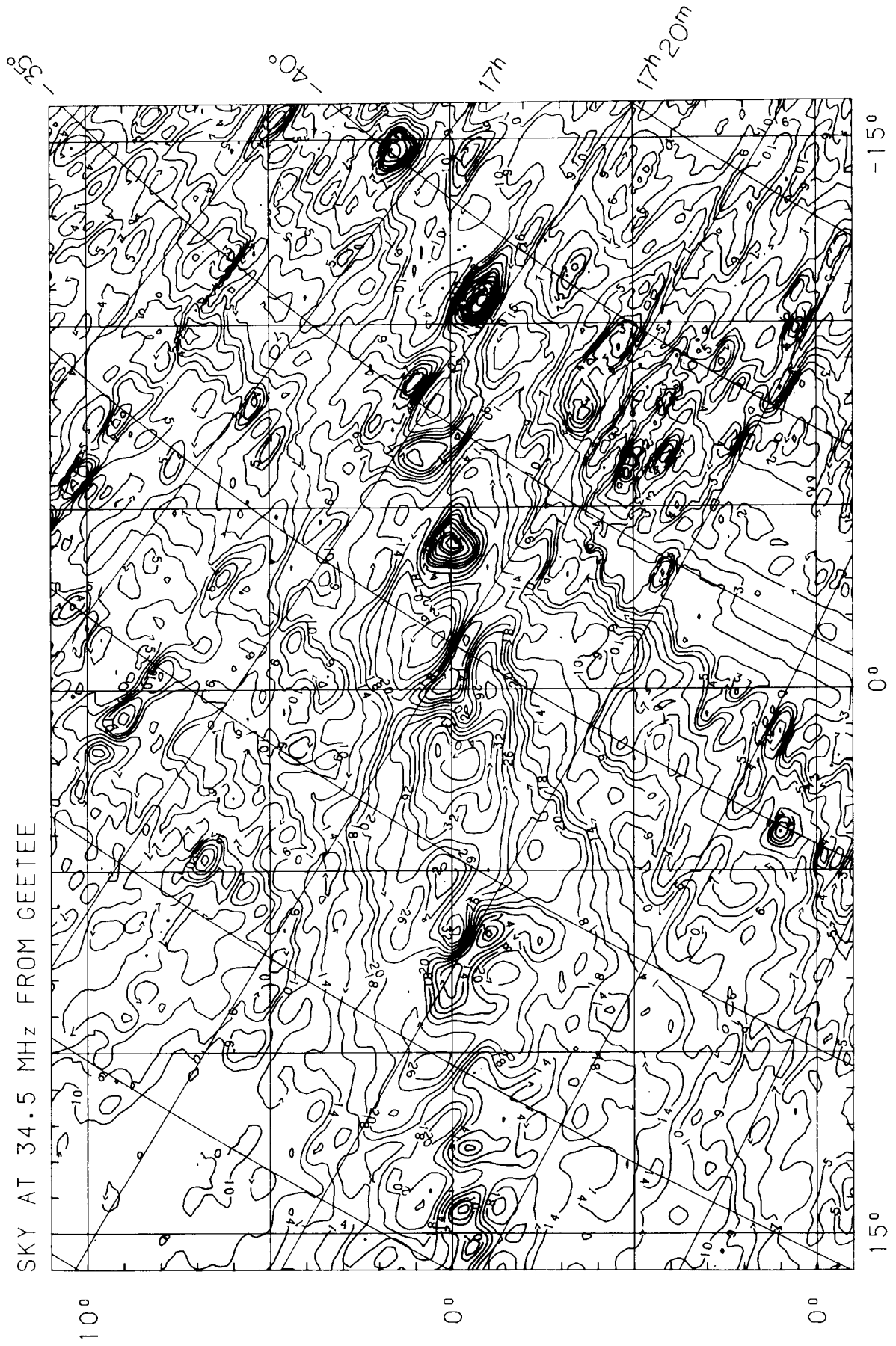
6.2.1 Signal-to-noise ratio in the maps

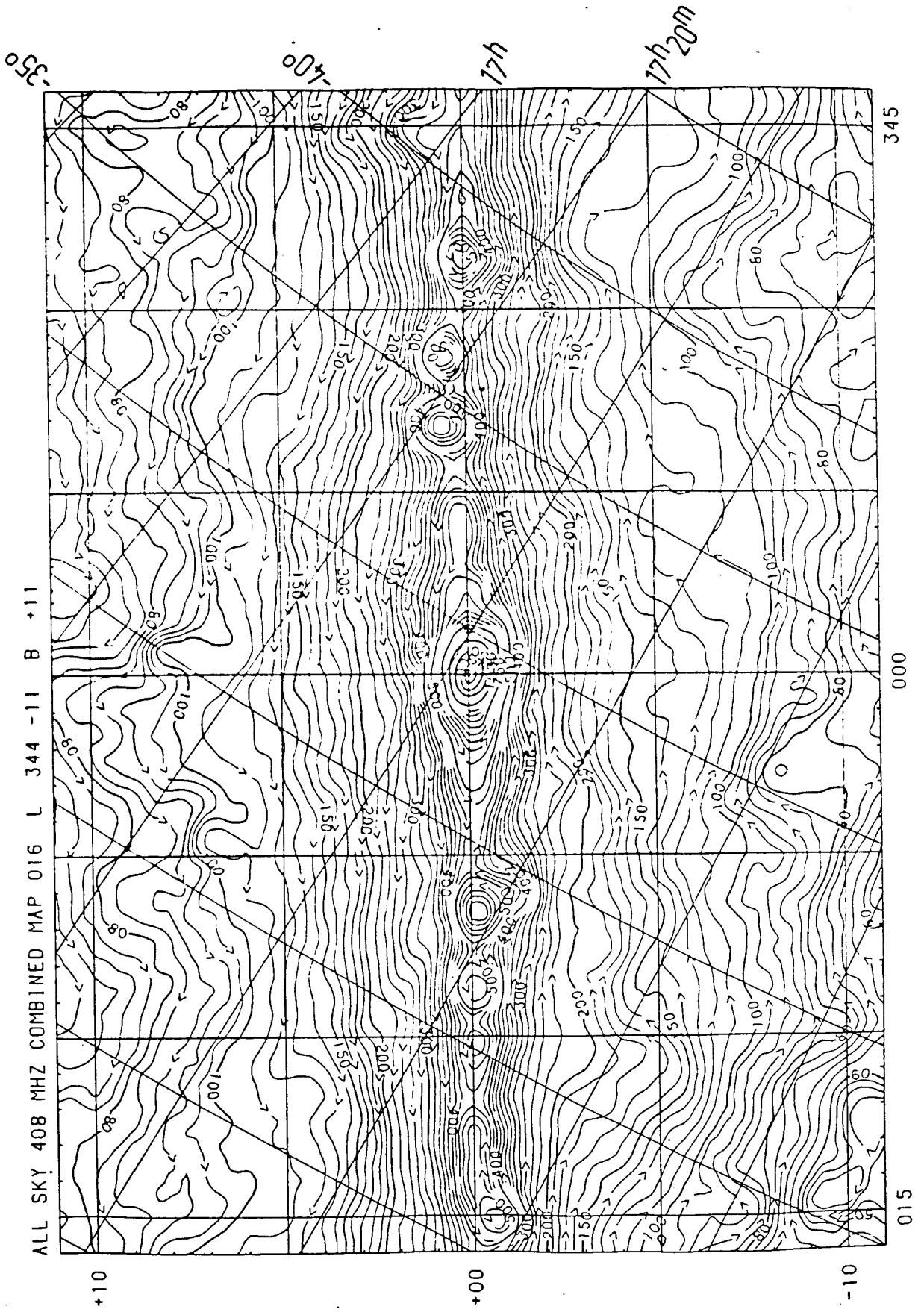
To estimate the signal to noise ratio (**S/N**) in the two maps (34.5 MHz and 408 MHz) of the same region, consider, for example, the map centered at $l = 150^\circ$. The value of the background at $b = +10^\circ$ is $\approx 2.3 \times 10^4 \text{ K}$ at 34.5 MHz and $\approx 40 \text{ K}$ at 408 MHz. The system noise in the 34.5 MHz map is $\approx 1.6 \text{ Jy}$ (or $\approx 700 \text{ K}$) implying a **S/N of ≈ 30** . Convolution of the 34.5 MHz map to the resolution of the 408 MHz map improves the S/N from 30 to 40. In the 408 MHz map, the system noise is $\approx 0.7 \text{ K}$ (C.J. Salter, personal communication) implying a S/N of ≈ 60 . Thus, there is no significant difference in the S/N ratios in the two maps; this is confirmed by the similar appearance of the two maps when convolved to the same resolution of $51' \times 51'$.

6.2.2 The paucity of point sources towards the inner Galaxy

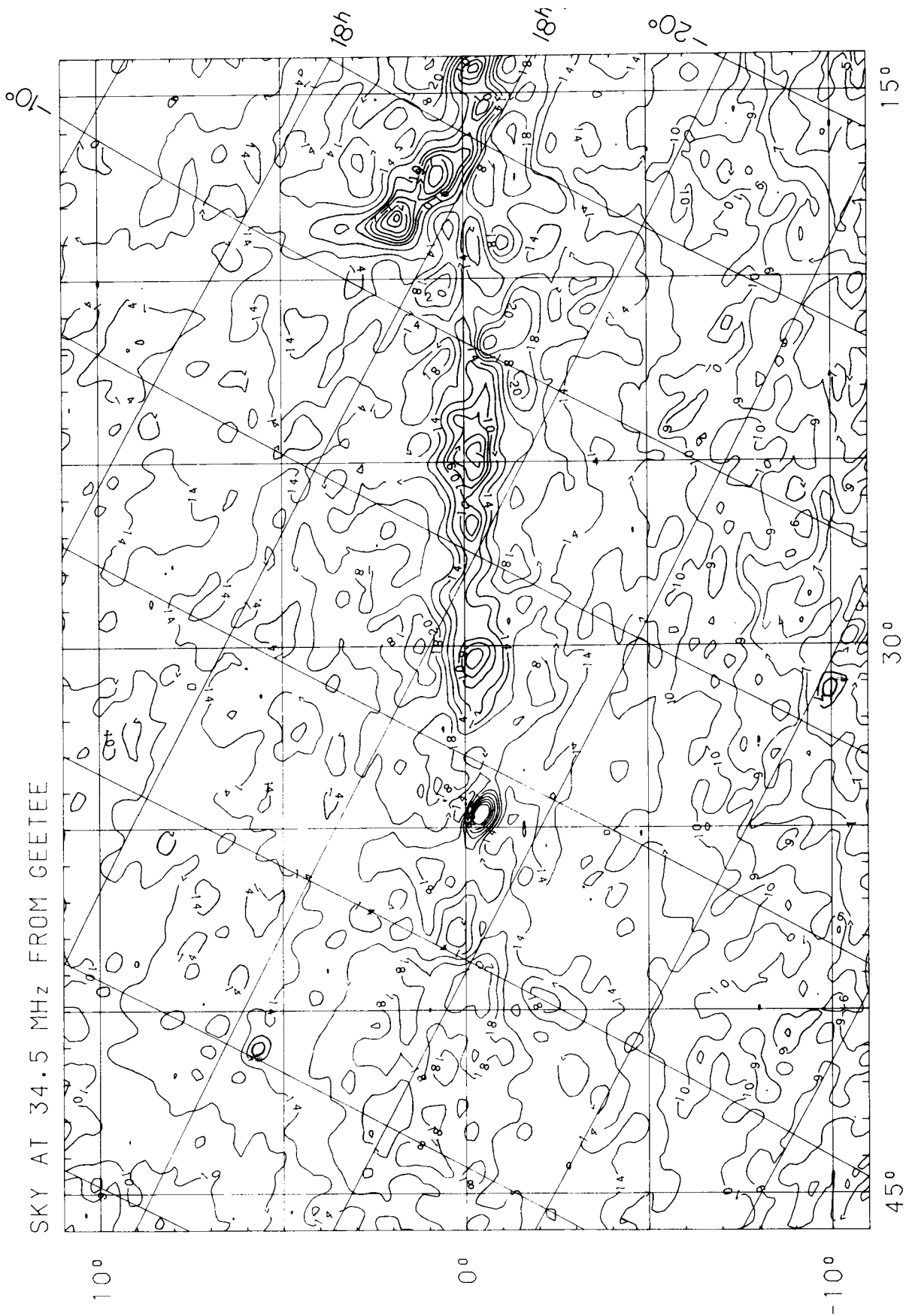
Point sources can be recognised on the 34.5 MHz maps by the

SKY AT 34.5 MHz FROM GEETEE

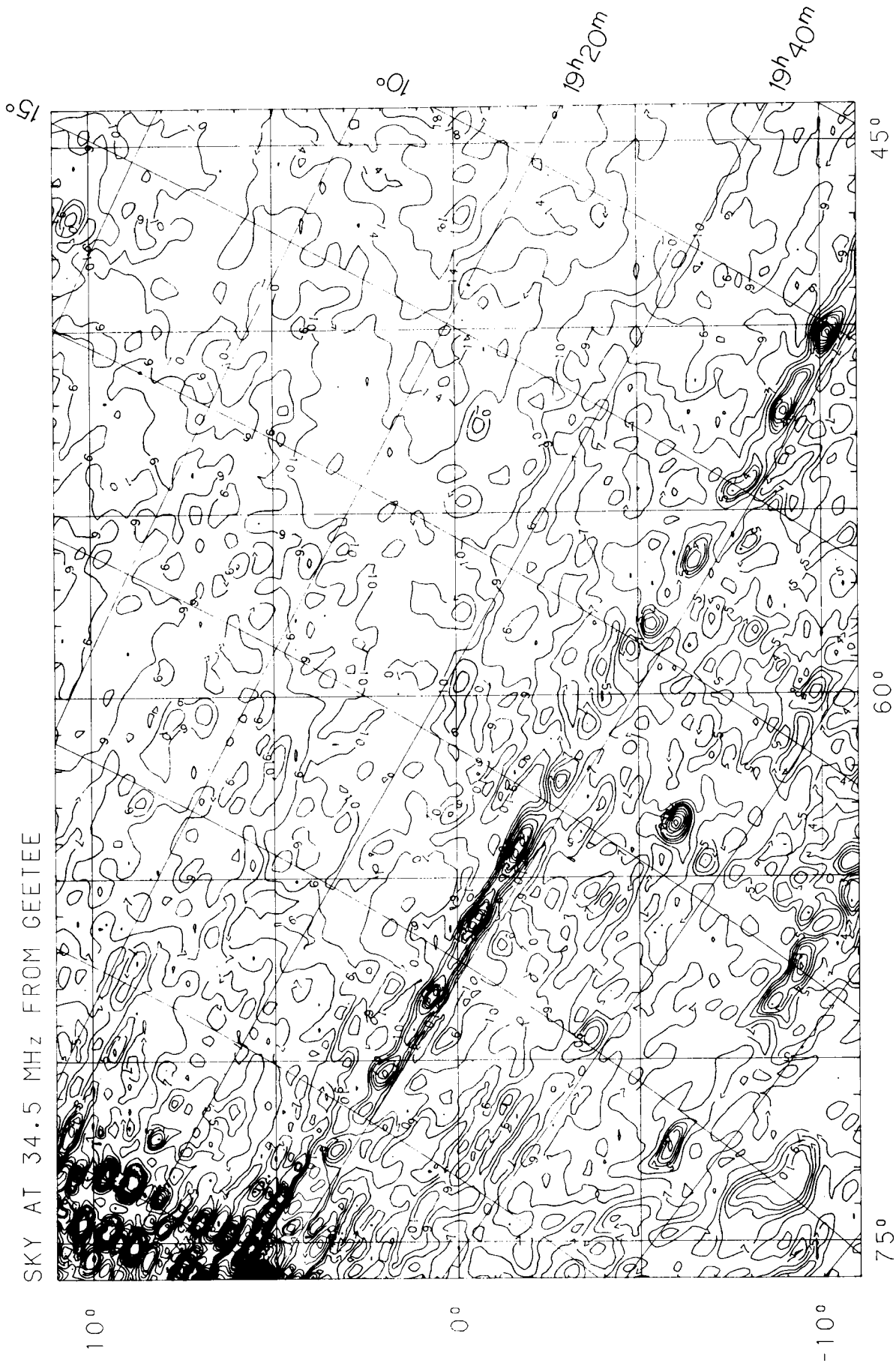




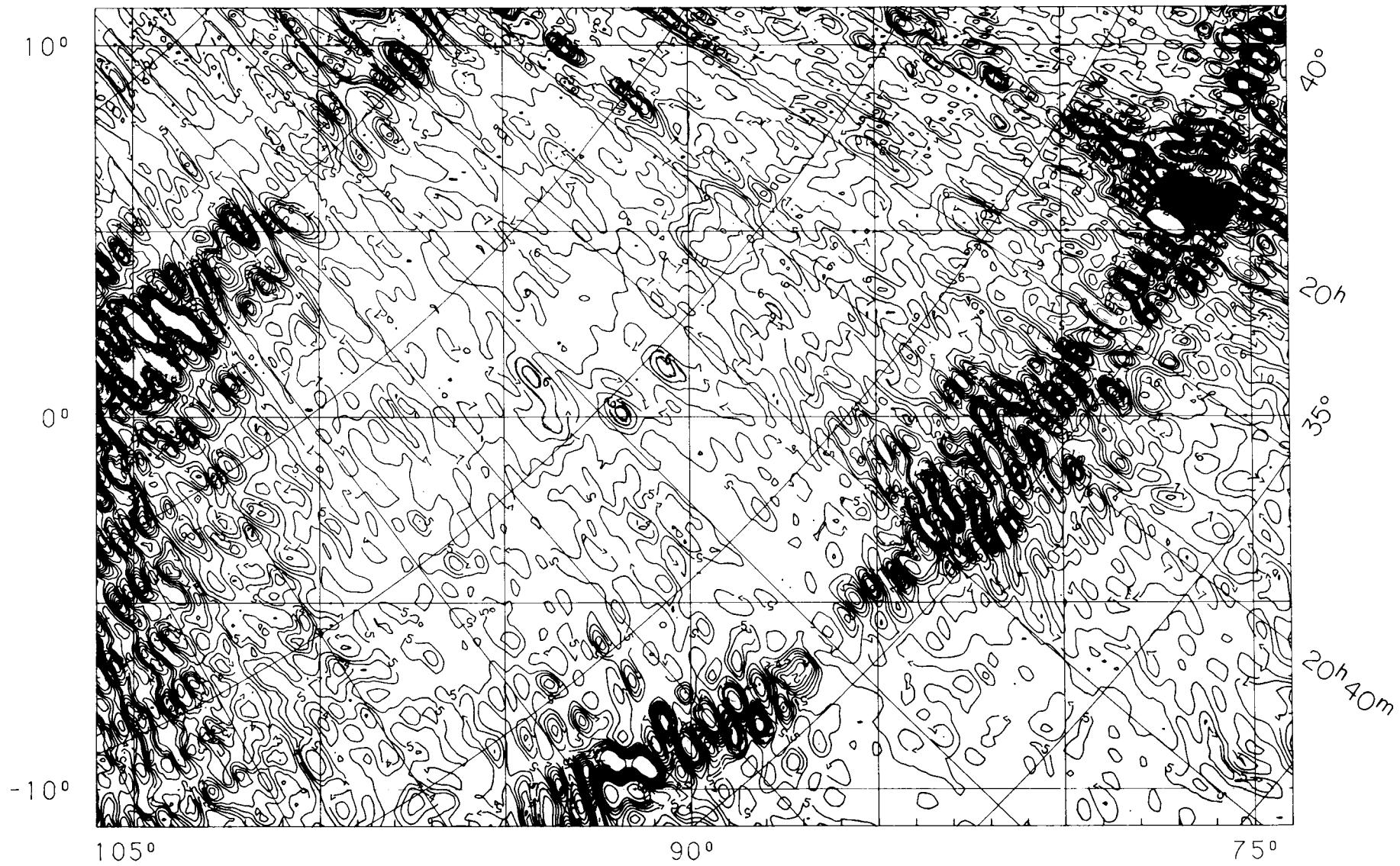
SKY AT 34.5 MHz FROM GEETEE

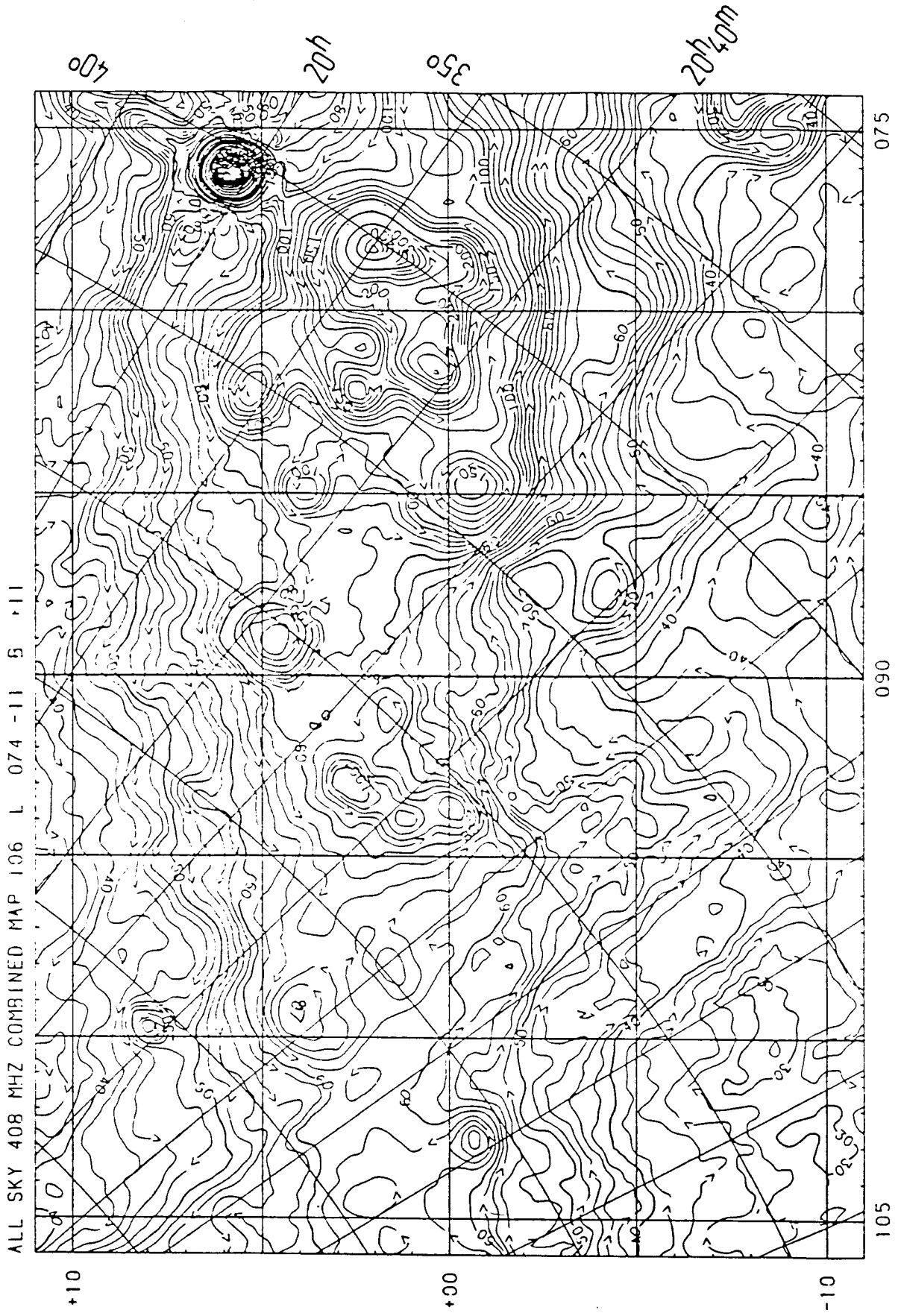


SKY AT 34.5 MHz FROM GEETEE

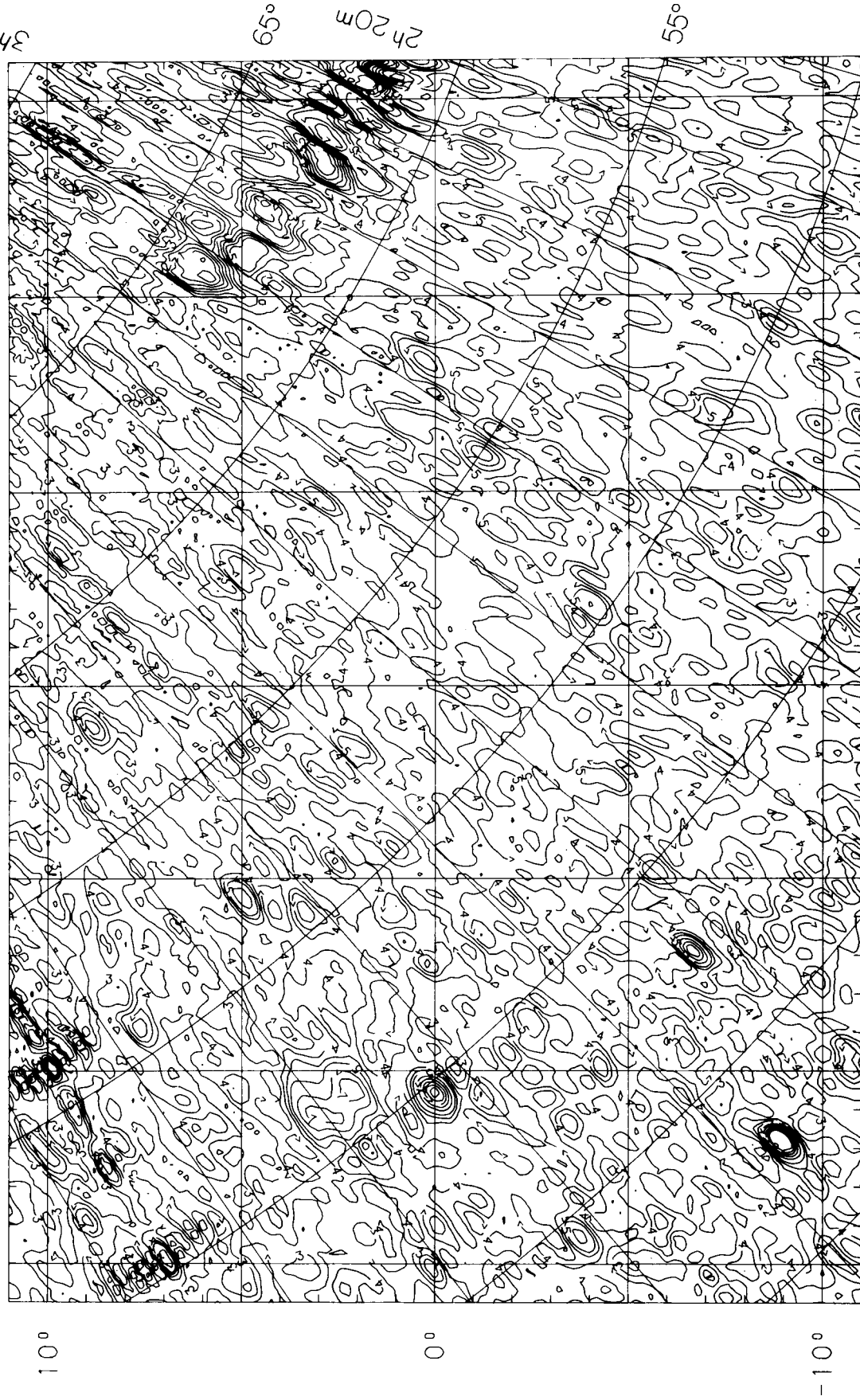


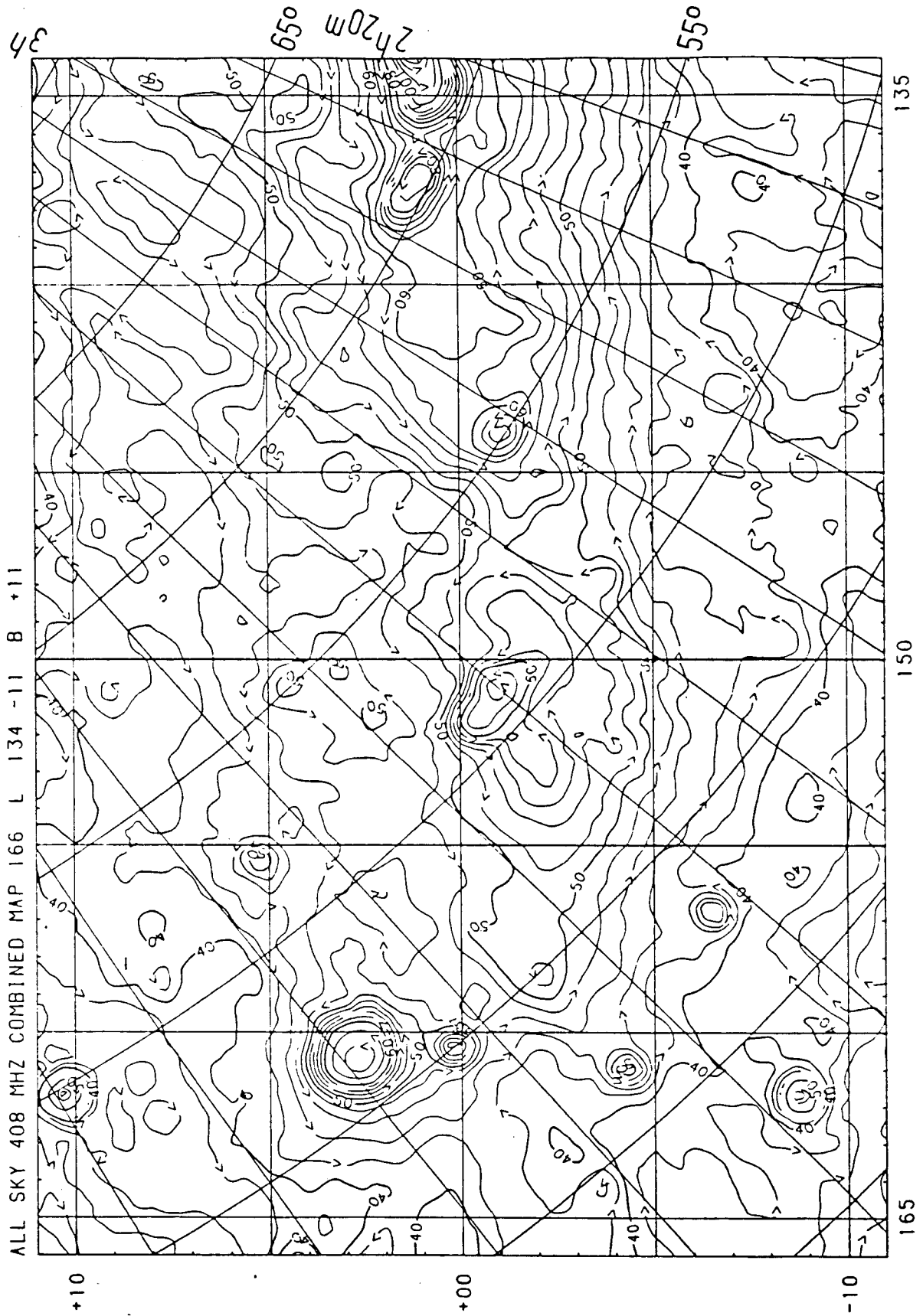
SKY AT 34.5 MHz FROM GEETEE



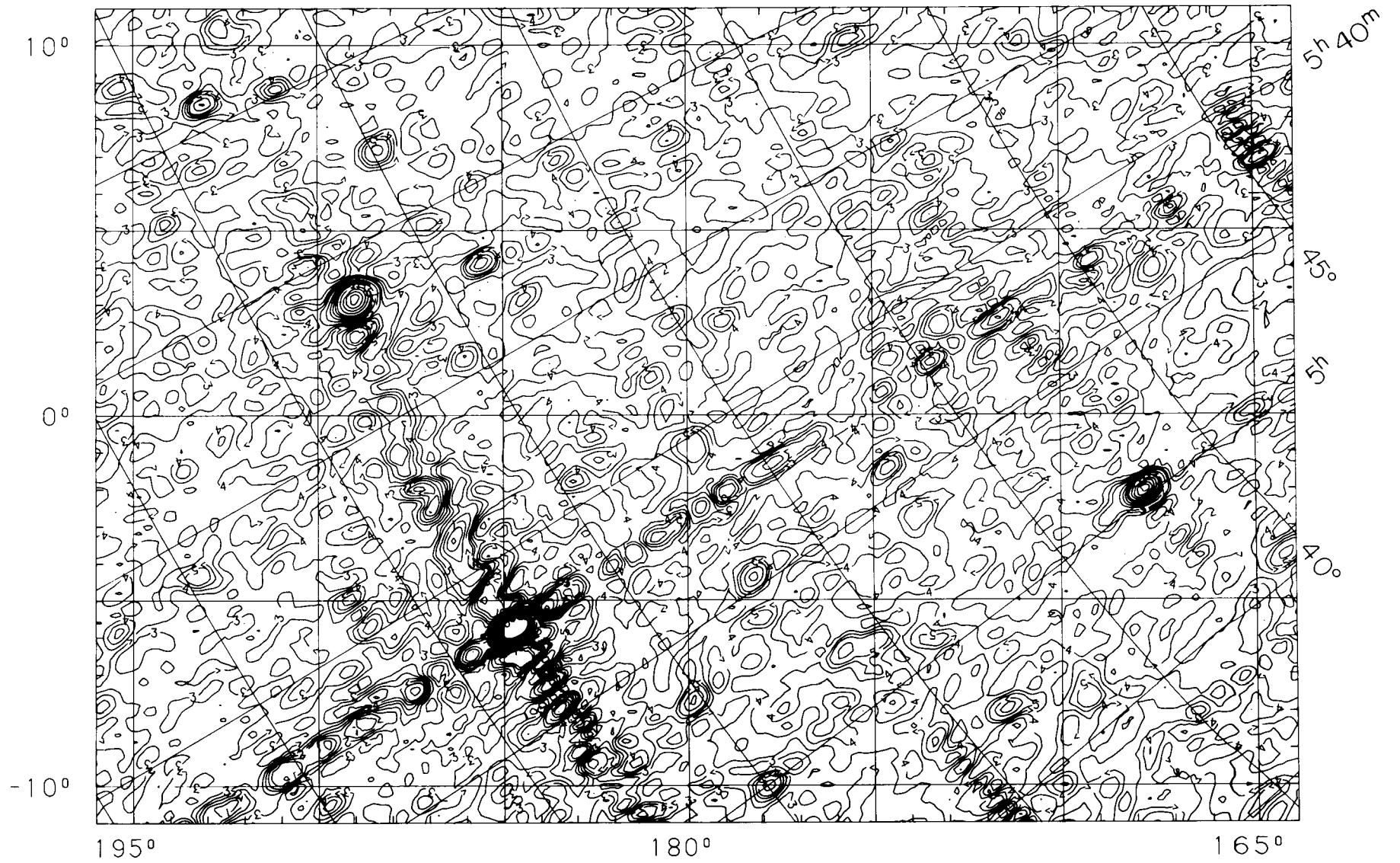


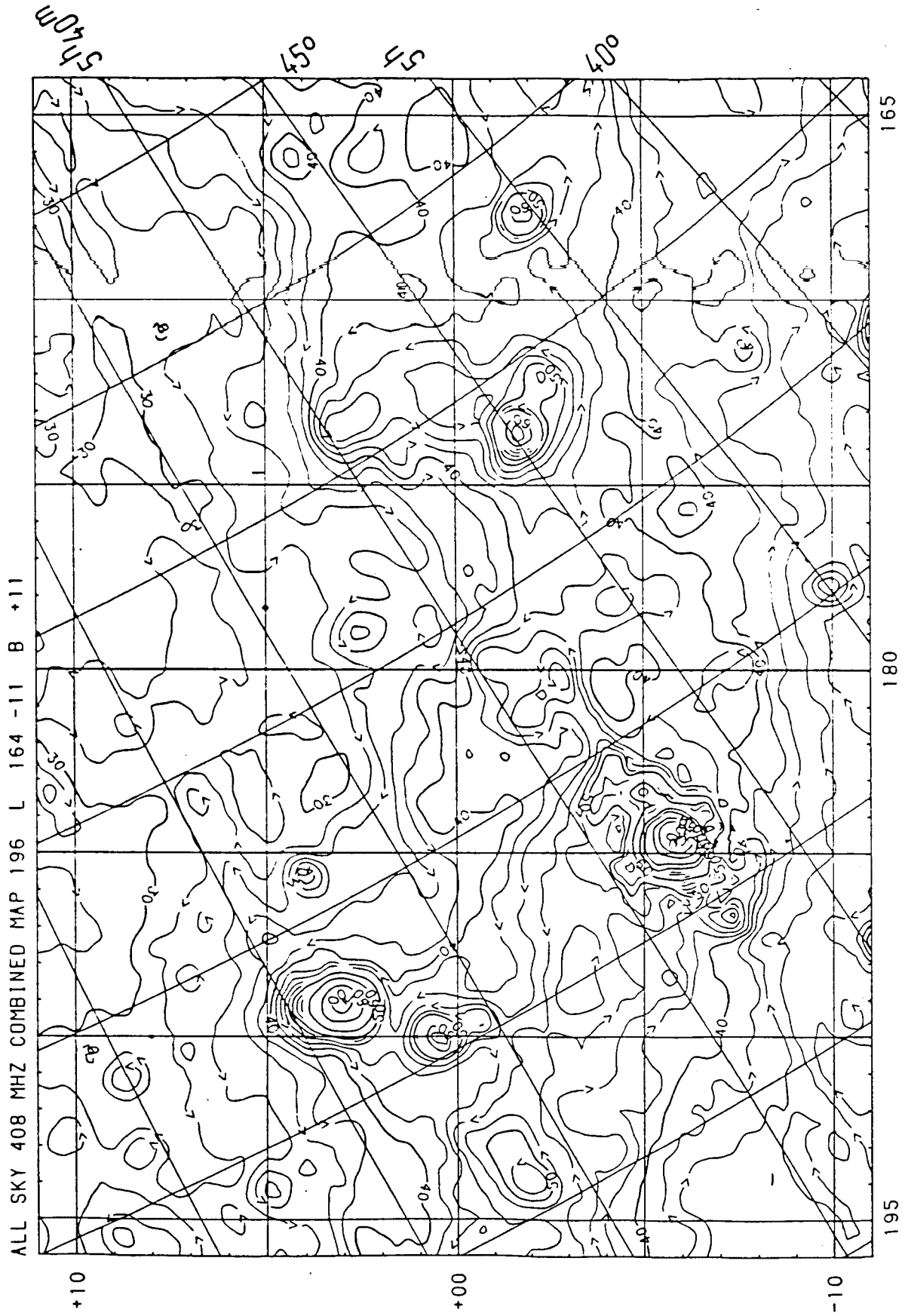
SKY AT 34.5 MHz FROM GEETEE



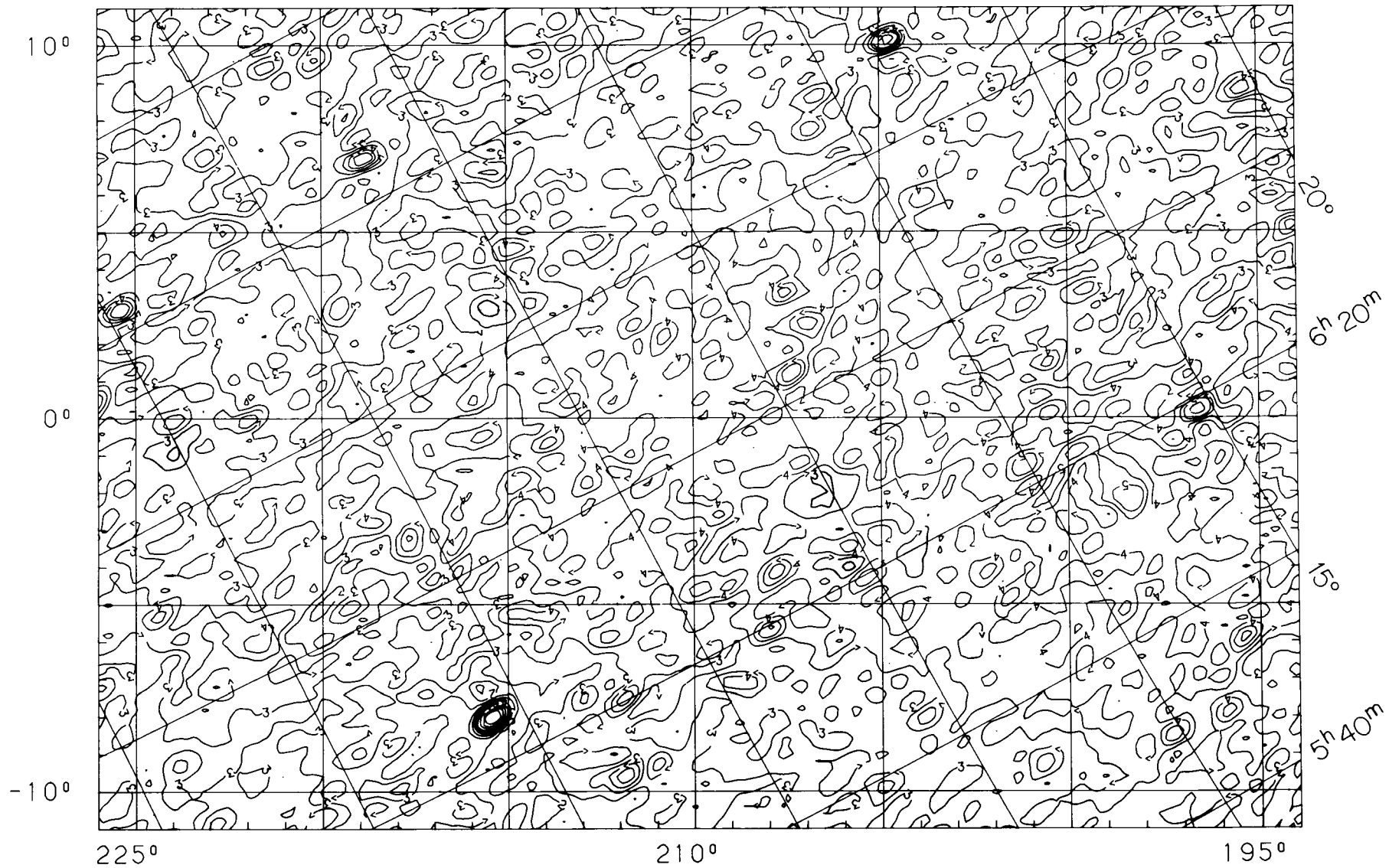


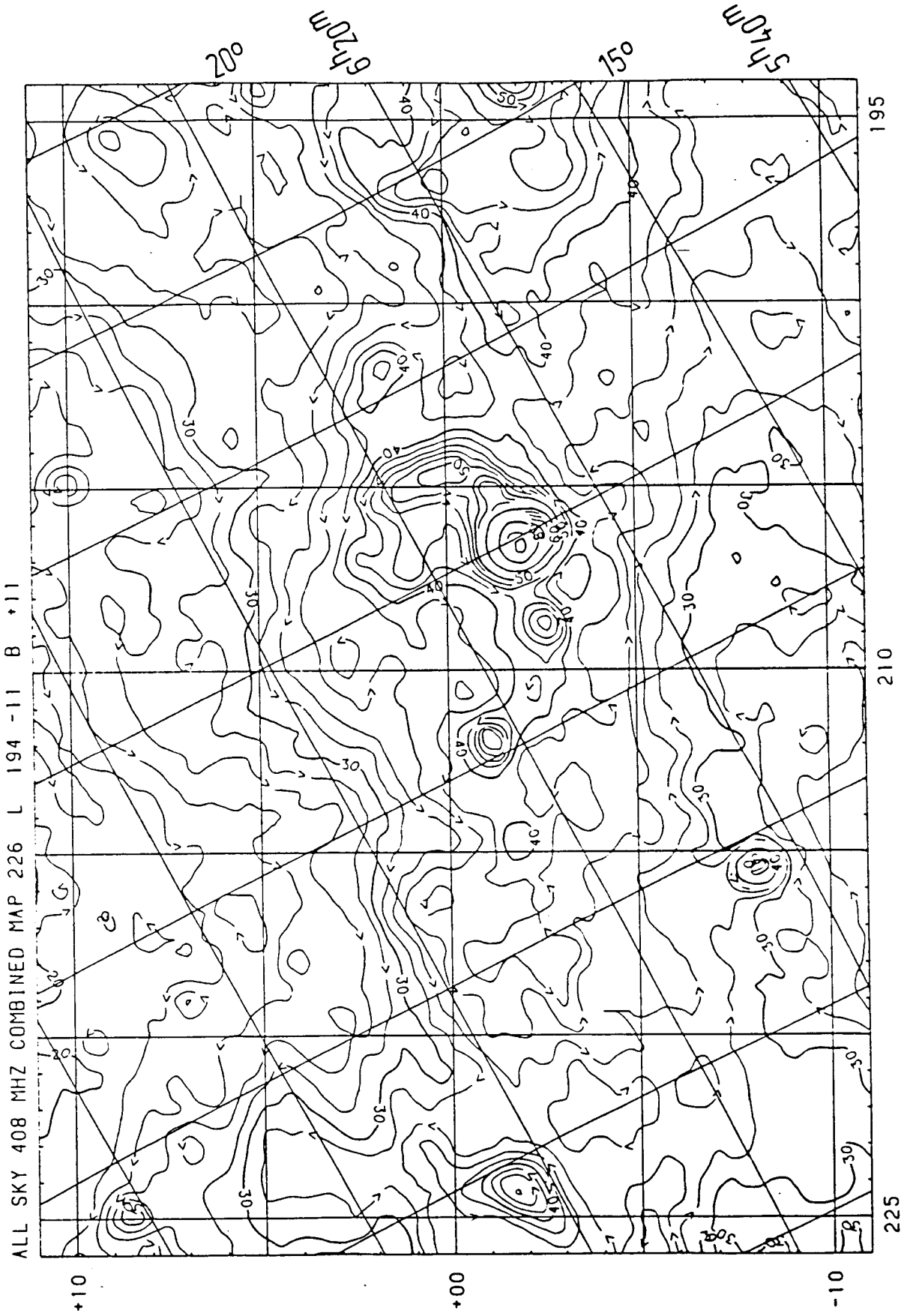
SKY AT 34.5 MHz FROM GEETEE



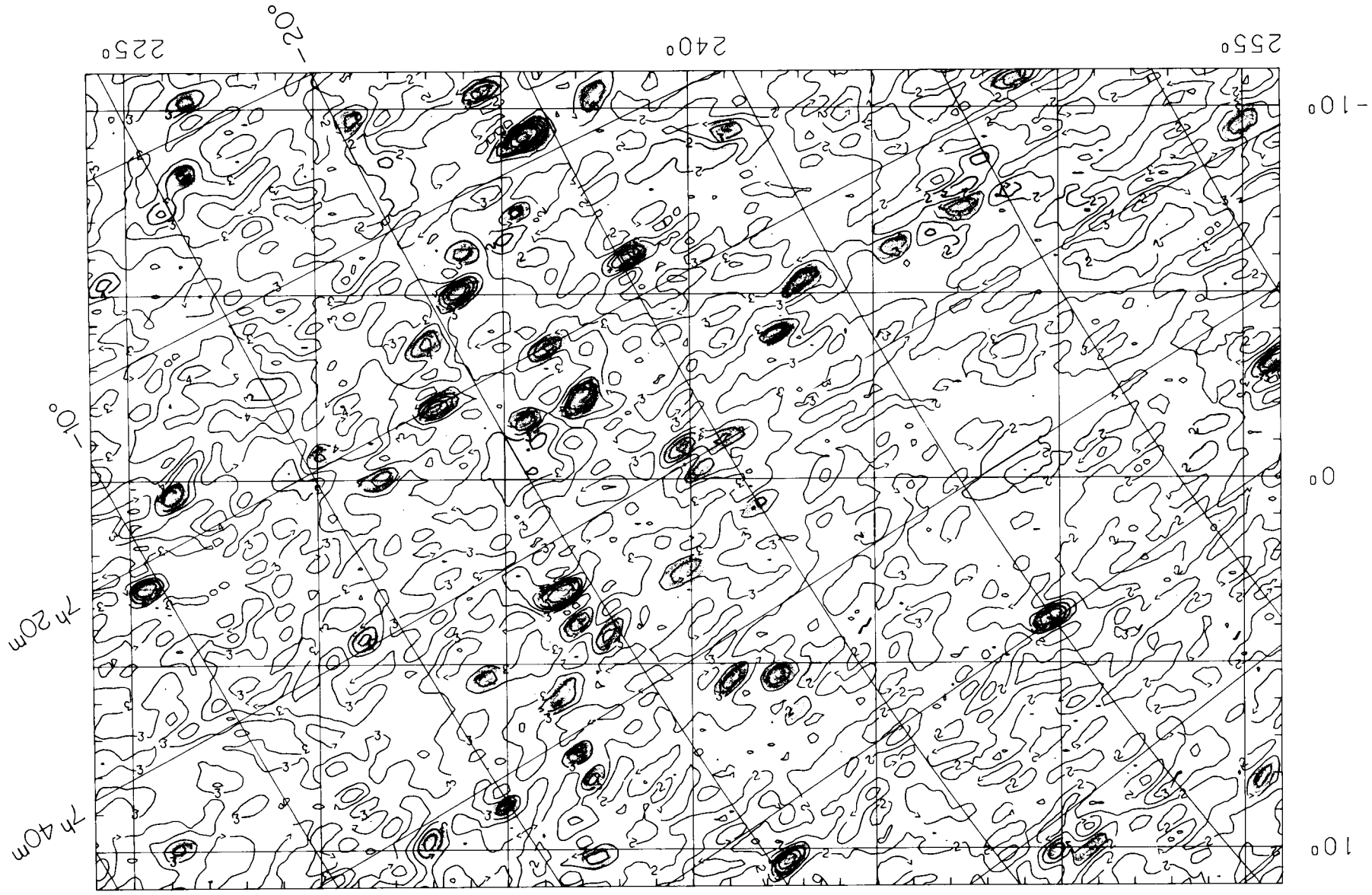


SKY AT 34.5 MHz FROM GEETEE

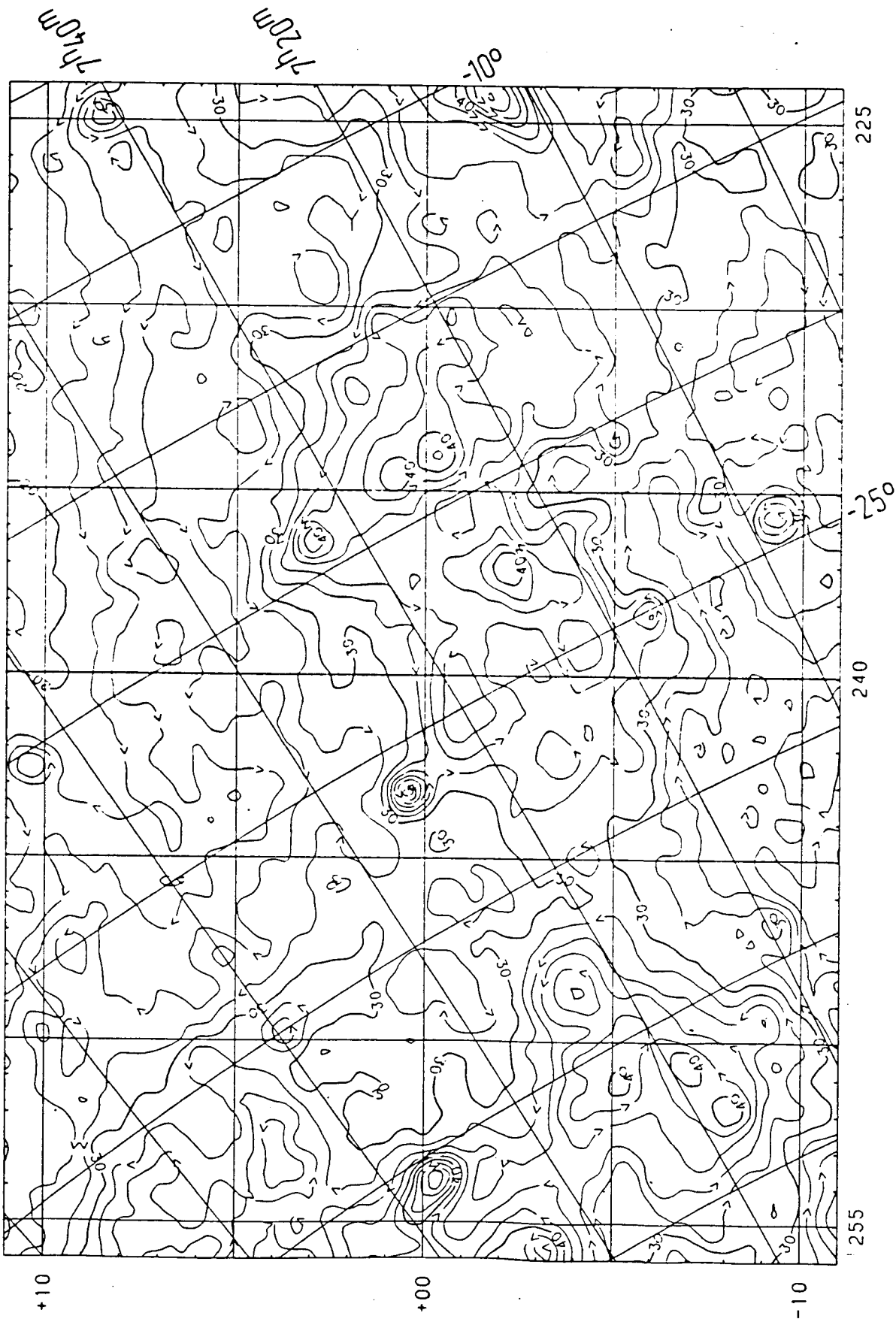




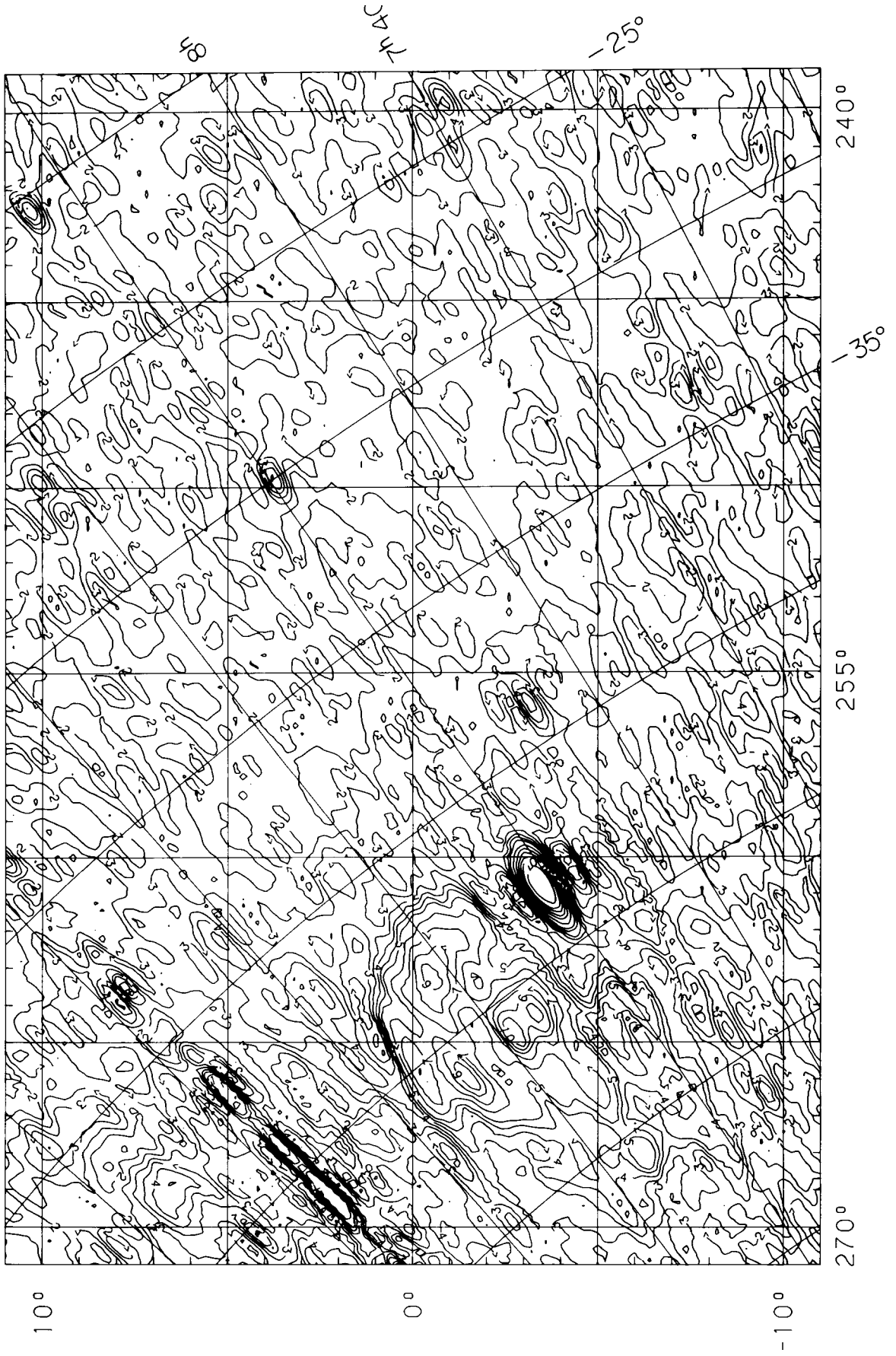
SKY AT 34.5 MHz FROM GEETEE

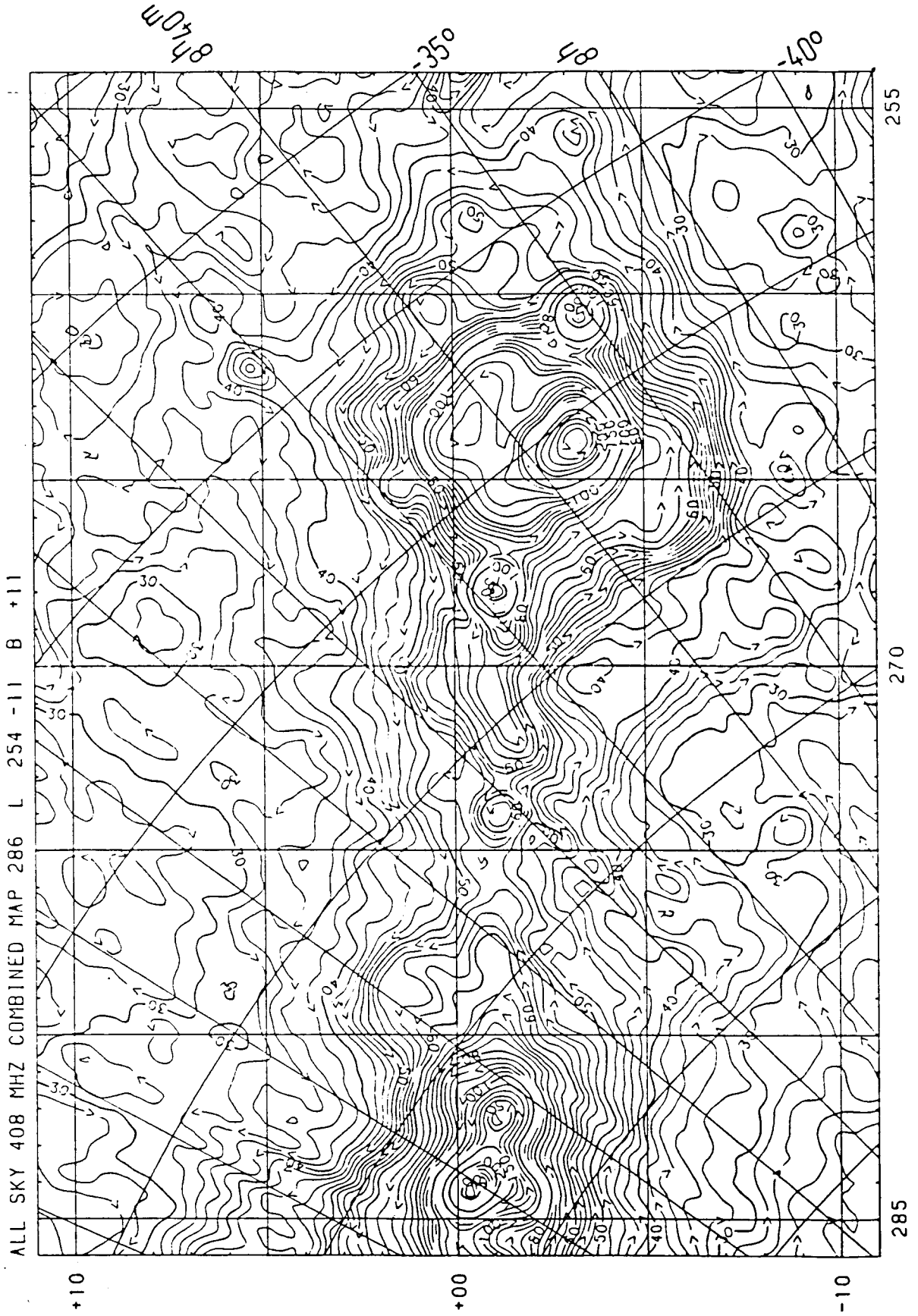


ALL SKY 408 MHZ COMBINED MAP 256 L 224 -11 B +11



SKY AT 34.5 MHz FROM GEETEE





orientation and size of the antenna beam they display. In this context 'point sources' are those whose angular sizes are small compared to the full width at half maximum of the main beam of the telescope. Most of the point sources on the maps are extragalactic sources (these are marked in pink colour on the maps centered at $l=240^\circ$ and $l=30^\circ$). As one moves from the outer Galaxy to the inner Galaxy the number density of sources seen within the $\pm 10^\circ$ latitude range decreases dramatically. Compare, for example, the map centered at $l = 240^\circ$ with that centered at $l = 30^\circ$. There are ≈ 50 point sources in the map shown centered at $l = 240^\circ$ while there are only 2 point sources in the map centered at $l = 30^\circ$. Even after allowing for the slightly increased noise towards the Galactic plane, the difference is very large. This is again indicative of the absorption in the disc of the 'Galaxy.

6.2.3 Discrete absorptions in the Galactic plane

As may be seen from the 34.5 MHz maps the equivalent black-body temperature of the non-thermal background ranges from 20,000 K towards the Galactic anticentre direction to 100,000 K towards the Galactic centre direction. The typical temperatures of HII regions lie in the range of 5000 K - 10000 K. Thus, under suitable circumstances (as will be described in the next section) the cooler HII regions appear in absorption against the hotter background. This phenomenon occurs predominantly at low frequencies. For example, an HII region with an electron temperature of 5000 K and an emission measure of $1000 \text{ cm}^{-6} \text{ pc}$ has an optical depth of 1 at 34.5 MHz. As one moves to higher frequencies, the background temperature falls very rapidly and

the **HII** regions are seen in emission, At **408** MHz, for example, the galactic background varies from **40K** to **400K** and the **HII** regions appear in emission.

Several discrete absorption features can be seen in the **34.5** **MHz** maps - predominantly in the longitude ranges of $345^\circ < l < 50^\circ$ and $200^\circ < l < 250^\circ$. They can be recognised by the contour labels or arrows going clockwise (these are highlighted in yellow for easy recognition). The same sources can be seen in emission in the **408** MHz maps. The inner Galaxy is characterised by deep absorption features, while the outer Galaxy has only weaker ones. The absorption features towards the inner Galaxy are discussed in detail in the next section.

6.3 DISCRETE ABSORPTIONS - A DISCUSSION

We would like to focuss our attention here on the prominent absorption features that are seen in the longitude range $345^\circ < l < 40^\circ$, and in the latitude range $|b| < 5^\circ$. Table 6.1 gives the observed parameters for all these absorption regions. Table 6.2 gives their associated optical nebulosities and their distance estimates.

6.3.1 Distances and the electron densities of the absorption features

One can estimate the limits to the electron densities and to the distances of the sources that produce the discrete absorption features from the fractional absorptions that we see against them, Consider the following two equations:

$$T_{\text{off}} = T_b + T_f \tag{6.1}$$

Table 6.1 Observed angular sizes (corrected for beam broadening) and average fractional absorptions of the discrete absorption features seen in the inner Galaxy. Sizes are as measured along r.a. x dec.. The size in dec. of 0.8 is only an upper limit as in these cases there is no significant beam broadening. Galactic coordinates refer to the centroid of the absorption feature.

l (deg.)	b (deg.)	size (deg.)	T_{off} (10^4 K)	$\langle \Delta T \rangle$ (10^4 K)	$\langle \Delta T \rangle / T_{off}$
345.4	+ 1.5	1.1 x 1.1	4	3.3	0.83
345.5	- 0.5	0.4 x 1.4	5.7	1.8	0.32
349.4	- 0.8	0.7 x 1.4	5.2	4.5	0.86
350.7	- 4.6	0.6 x 0.8	2.3	0.8	0.36
351.6	+ 1.0	0.4 x 0.8	8.0	6.6	0.83
352.5	- 3.6	0.6 x 0.8	2.3	1.3	0.57
353.7	+ 1.0	0.8 x 0.8	5.7	5.4	0.95
356.0	+ 0.0	1.4 x 1.5	8.0	3.7	0.46
359.8	+ 0.0	0.4 x 2.1	21.7	12.3	0.57
5.4	+ 0.2	0.8 x 1.1	15.0	7.0	0.47
6.8	- 1.0	0.8 x 1.0	10.0	7.5	0.75
6.9	- 2.4	1.1 x 0.8	10.0	7.8	0.78
8.0	+ 0.0	2.1 x 1.3	10.0	4.2	0.42
8.8	- 4.3	0.7 x 0.8	8.6	3.6	0.42
10.6	- 0.6	0.6 x 0.8	11.4	10.1	0.89
11.1	- 2.0	0.6 x 1.4	8.0	1.1	0.14
12.7	- 0.4	1.1 x 1.2	8.5	4.5	0.53
14.4	- 0.3	0.8 x 1.3	9.2	1.4	0.15
15.4	- 0.5	0.4 x 0.8	9.1	2.5	0.27
17.2	+ 0.7	1.3 x 1.8	8.0	4.7	0.58
18.3	+ 1.8	1.2 x 1.3	8.0	5.2	0.65
19.1	- 0.3	0.4 x 0.8	10.3	7.9	0.76
24.7	- 0.3	2.0 x 2.8	9.1	4.8	0.53
26.7	- 0.2	1.0 x 1.4	9.1	7.9	0.87
30.4	- 0.3	1.6 x 2.3	9.1	6.0	0.66
37.9	+ 0.3	0.7 x 1.4	9.1	2.6	0.29

$$T_{on} = T_b e^{-\tau} + T_e (1 - e^{-\tau}) + T_f \quad (6.2)$$

Where,

T_{off} is the observed brightness temperature outside the source (absorption feature or the **HII** region),

T_{on} is the observed brightness temperature on the source,

T_b is the contribution from behind the **HII** region,

T_f is the contribution from the near side of the **HII** region,

τ is the free-free optical depth of the **HII** region, and

T_e is the electron temperature of the **HII** region.

From equations 6.1 and 6.2 we find,

$$\Delta T = T_{on} - T_{off} = (T_e - T_b) (1 - e^{-\tau}) \quad (6.3)$$

Assuming uniform emissivity for the galactic non-thermal background, we get, $T_{off} = K \times L$ where, K is the non-thermal emissivity of the galactic background (in, say, $K \text{ pc}^{-1}$) and L is the total length of the Galaxy along the line of sight (in **pc**). If the distance to the **HII** region is d , then,

$$\frac{\Delta T}{T_{off}} = \left(\frac{T_e}{T_{off}} - 1 + \frac{d}{L} \right) (1 - e^{-\tau}) \quad (6.4)$$

If the solid angle subtended by the **HII** region is Ω_s and that of the beam is Ω_{beam} , then,

$$(\Delta T)_{obs} = \Delta T \frac{\Omega_s}{\Omega_{beam}} \quad \text{for } \Omega_s \leq \Omega_{beam} \quad (6.5)$$

and,

$$(\Delta T)_{obs} = \Delta T \quad \text{for } \Omega_s > \Omega_{beam} \quad (6.6)$$

The free-free optical depth is given by (Altenhoff et al. 1960),

$$\tau = 0.08235 T_e^{-1.35} \nu^{-2.1} \int_0^l n_e^2 dl \quad (6.7)$$

where,

T_e is the electron temperature in K,

ν is the frequency of observation in GHz,

n_e is the electron density in cm^{-3} , and

l is the thickness of the gas in pc.

Thus, given a certain linear size of the HII region and its distance, AT can be calculated for a given T_{off} , T_e and n_e . It follows from eqs. (6.4), (6.5) and (6.6) that the present survey will be more sensitive to the nearby and bigger HII regions, since the effects of beam dilution and foreground emission will be less important for these.

Figures 6.5, 6.6 and 6.7 show curves of constant $(\Delta T)_{\text{obs}}/T_{\text{off}}$ as a function of the size of the HII region and its distance from the sun for three different electron densities - $n_e = 4 \text{ cm}^{-3}$, 8 cm^{-3} and 16 cm^{-3} . An electron temperature of 8000 K has been assumed in all these. These curves are drawn for a $T_{\text{off}} = 10^5 \text{ K}$ and are appropriate for most of the HII regions listed here. If the electron density is increased further, except for a crowding of the curves near the bottom left hand corner of the plot, it remains essentially unaltered. The three broken lines represent the relation between the linear size and the distance for three angular diameters of 0.5° , 1° and 2° . It can be seen from Table 6.1 that most of the HII regions have angular diameters in this range.

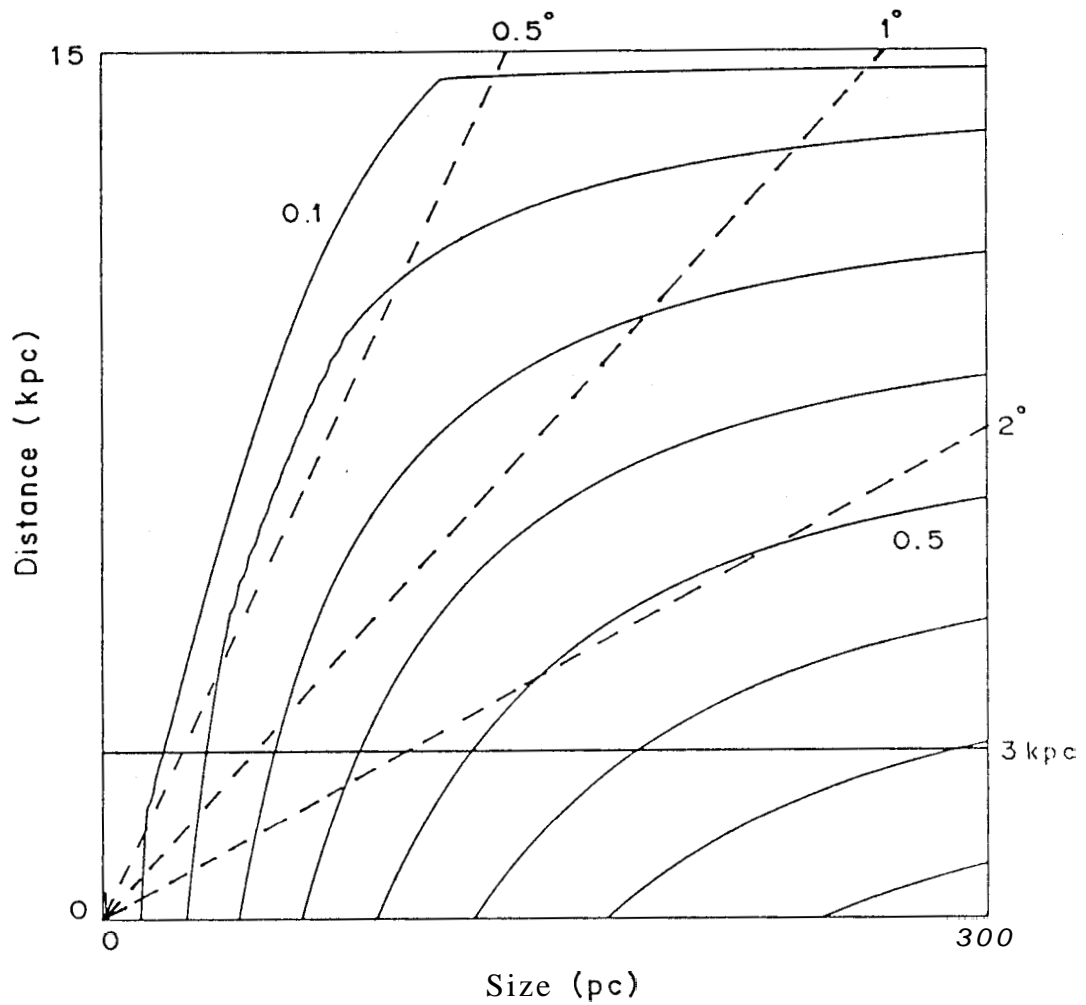


Fig. 6.5: Curves of fractional absorption (computed on the basis of the eqs. 6.5 and 6.6) as a function of the distance to the HII region and its linear size. These curves are appropriate for a $T_{\text{off}} = 10^5$ K, $T_e = 8000$ K and $n_e = 4 \text{ cm}^{-3}$. The broken lines represent the limits on the sizes and distances as implied by the observed angular sizes of the discrete absorptions seen on our map. Most of these absorptions are also within 3 kpc from the sun as implied by their correspondences with the $H\alpha$ nebulosities.

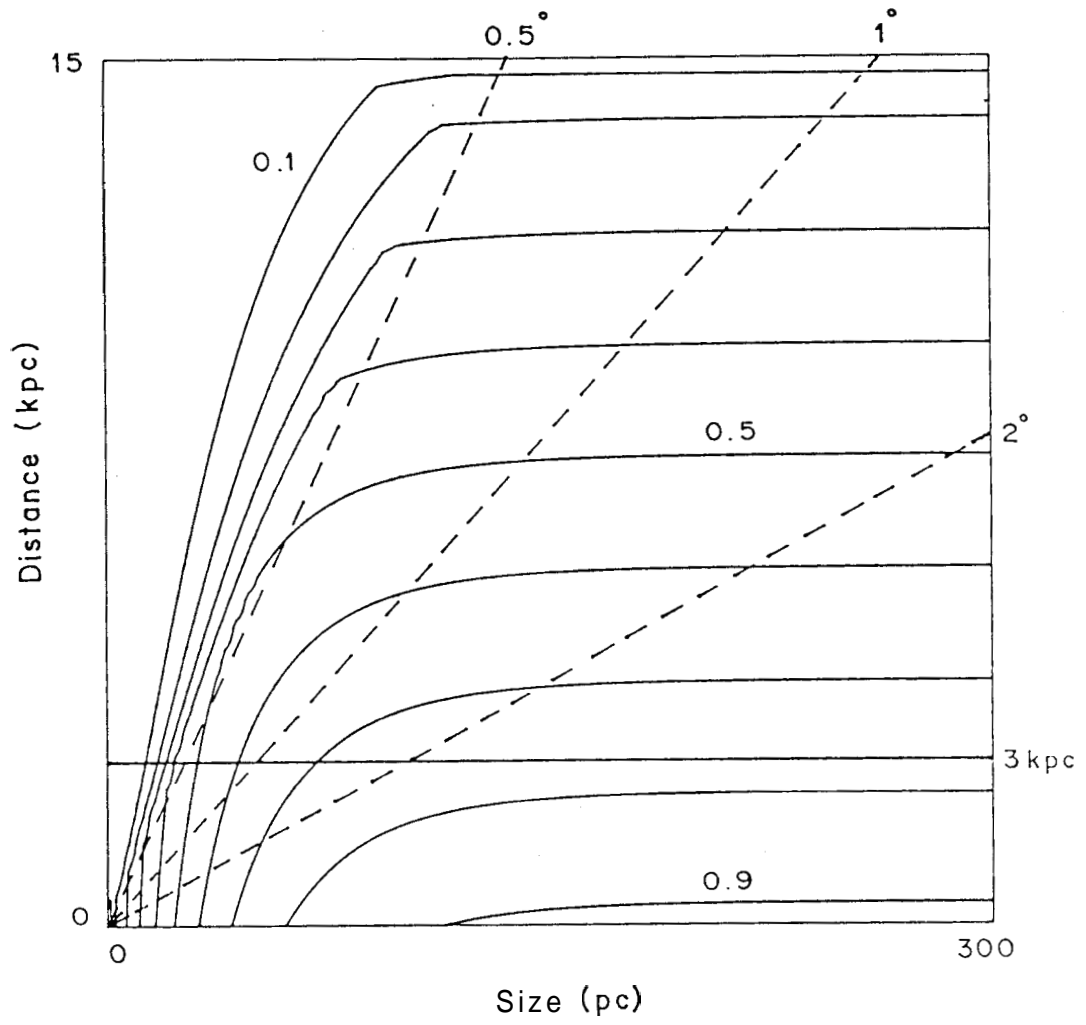


Fig. 6.6: Same as Fig. 6.5 but for an $n_e = 8 \text{ cm}^{-3}$

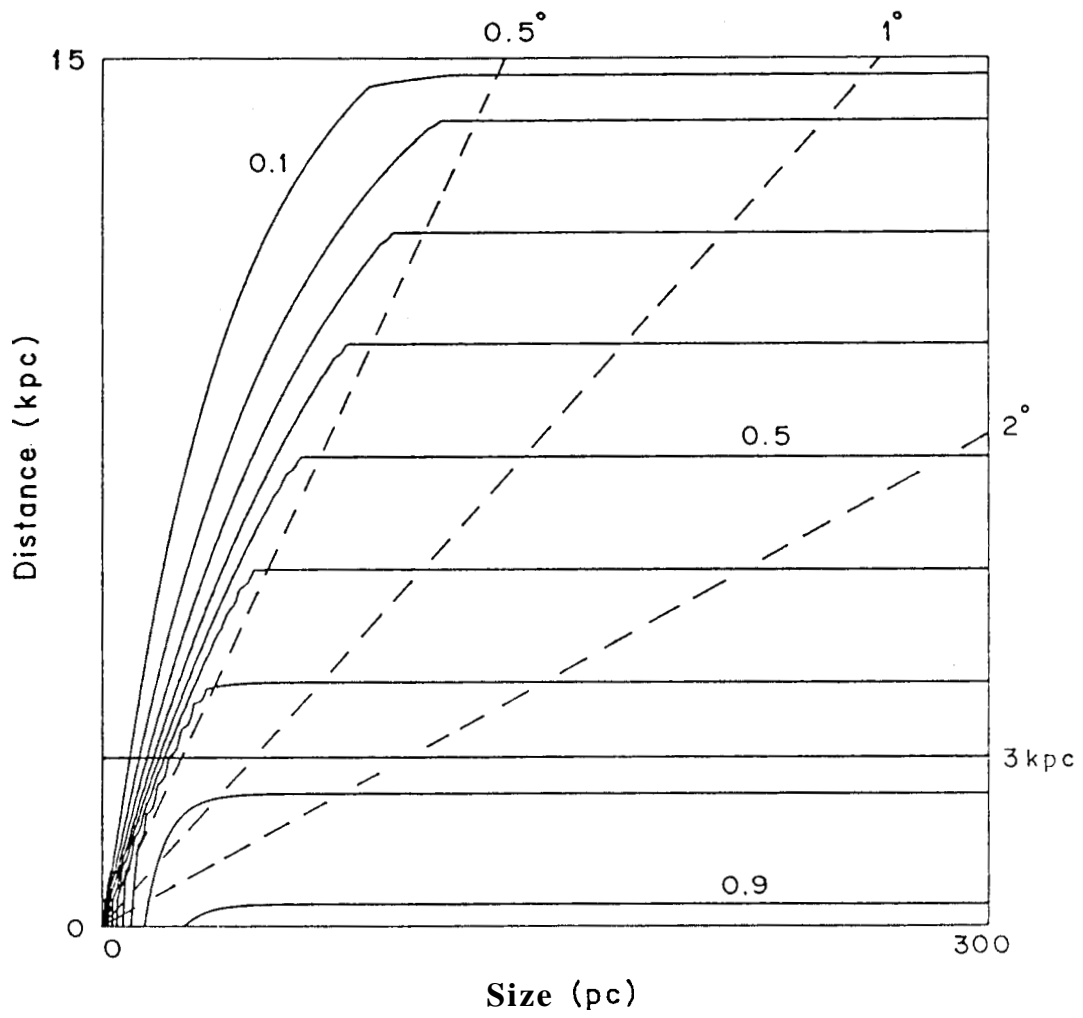


Fig. 6.7: Same as Fig. 6.5 but for an $n_e = 16 \text{ cm}^{-3}$

An examination of the last colouan of Table 6.1 shows that in the majority of cases the observed value of $\langle \Delta T \rangle / T_{\text{off}}$ is greater than 0.4. Using these as constraints one can conclude that the electron densities in most of these HII regions must be $> 8 \text{ cm}^{-3}$ (see figures 6.5 - 6.7). These figures also show that the HII regions with $\langle \Delta T \rangle / T_{\text{off}} > 0.6$ must be within 6 kpc from us.

In making the above estimates we have assumed $T_{\text{off}} = 10^5 \text{ K}$. If T_{off} is smaller (ex. $2 - 5 \times 10^4 \text{ K}$) then it follws that even the HII regions with smaller values of $\langle \Delta T \rangle / T_{\text{off}}$ (> 0.3) must be within 6 kpc.

6.3.2 Comparison with optical nebulosities

Table 6.2 lists the optical nebulosities that are most likely associated with the HII regions seen in the 34.5 MHz maps. Rodgers, Campbell and Whiteoak (RCW) have published a catalogue of the emission regions in the southern milky way (Rodgers et al. 1960). The RCW numbers refer to the source numbers in that catalogue. About half the number of the HII regions seen by us have associated RCW sources. The positional coincidence in almost all cases is better than 0.5° . The distances to several of these RCW sources are known through the work of Georgelin and Georgelin (1970), who have estimated the distances to the exciting stars associated with the RCW sources. These distances are also quoted in Table 6.2. It will be seen that wherever the distance estimate is available it is less than 3 kpc. This is to be expected since extinction due to dust precludes our seeing diffuse optical nebulosities far away. Apart from the formal coincidences of the RCW sources that are quoted in Table 6.2, a

Table 6.2 Optical correspondences of the discrete absorptions observed at 34.5 MHz. RCW refers to Rodgers et al. (1960) and Sivan refers to Sivan (1974). Distances are from Georgelin and Georgelin (1970). The galactic coordinates refer to the centroid of the discrete absorption observed at 34.5 MHz.

l (deg.)	b (deg.)	RCW no.	optical size (min. of arc)	distance (kpc)	Sivan
345.4	+ 1.5	-	-	-	Y
345.5	- 0.5	117	2 x 2	-	N
349.4	- 0.8	123	75 x 75	-	Y
350.7	- 4.6	-	-	-	Y
351.6	+ 1.0	127	50 x 25	1.51	Y
352.5	- 3.6	-	-	-	N
353.7	+ 1.0	131	170 x 55	1.58	Y
356.0	+ 0.0	132	110 x 80	1.38	Y
359.8	+ 0.0	137,138	-	-	Y
5.4	+ 0.2	-	-	-	Y
6.8	- 1.0	146	120 x 90	1.6	-
6.9	- 2.4	-	-	-	N
8.0	+ 0.0	148,149	120 x 30	-	-
8.8	- 4.3	-	-	-	Y
10.6	- 0.6	-	-	-	Y
11.1	- 2.0	151	100 x 35	1.82	Y
12.7	- 0.4	-	-	-	Y
14.4	- 0.3	157	60 x 60	-	Y
15.4	- 0.5	160	70 x 60	3.0	Y
17.2	+ 0.7	165	90 x 66	3.3	Y
18.3	+ 1.8	167	180 x 90	2.3	Y
19.1	- 0.3	166 ?	15 x 15	-	Y
24.7	- 0.3	172	7 x 7	2.5	Y
26.7	- 0.2	-	-	-	Y
30.4	- 0.3	176	8 x 8	3.0	N
37.9	+ 0.3	-	-	-	N

general statement can be made regarding the **HII** regions in the **34.5** MHz map and the RCW sources. There are a total of **50** RCW sources in the longitude range $345^\circ < l < 40^\circ$. Out of these **40** of them fall well within the boundaries of the absorptions. Furthermore, every discrete absorption at **34.5** MHz has at least one RCW source in it. While we are aware that not all RCW sources need be **HII** regions (some of them, like RCW 86, for example, are supernova remnants) their positional coincidence with the absorption features can be taken to indicate that the majority of the RCW sources are **HII** regions, and that these are fairly nearby. Ten of the RCW sources which do not have any associated absorption have angular diameters of $\approx 10'$ and are not expected to produce any detectable absorption.

Sivan (1974) has made a very-wide-field photographic **H α** survey of the milky way. This survey has detected many new extended areas of faint diffuse emission associated with the local and the Sagittarius arms. Assuming the temperature of the emitting gas to be **6000** K and making no extinction correction, Sivan estimates the limiting emission measure of his survey to be less than 30 cm^{-6} pc. The distances to several of these bright **H α** emission regions are known. If a correspondence between the **H α** emission patches and the **34.5** MHz absorptions is made firmer we will be able to get distance limits to more of the discrete absorptions than was possible with the RCW sources.

A comparison of the 2° resolution maps at **34.5** MHz and **408** MHz shows that the emission seen at $l = 173^\circ$ and $b = -2^\circ$ on the **408** MHz map is absent on the **34.5** MHz map (Fig. 6.3 and 6.4) indicating that it is a region of flat spectrum (compared to the

background emission). The higher resolution maps at 34.5 MHz show absorptions in this region. The **H α photograph** of Sivan shows a bright **H α emission** patch at the same position with very little **H α** emission outside of this region. This agreement is unlikely to be a coincidence.

In addition, we reproduce in Table 6.3 the coordinates, sizes and distances of the newly discovered regions of faint **H α** emission (Table 2 of Sivan 1974). The **H α** emission regions in this table with numbers **1,8,9** and 11 are clearly seen as absorption regions in the 34.5 MHz maps (see maps in Chapter 4 for regions 8 and 9). The regions 3,4 and 10 show an indication of absorption in the 34.5 MHz maps (see maps in Chapter 4). Region 2 falls in the disturbed region due to Cas A. Regions **5,6** and 7 do not show indications of absorption. The trend is clear. Only the three smallest regions have not been seen in the 34.5 MHz maps as absorptions. This, of course, is a question of sensitivity. The rest have been seen. In addition, in all those cases where the distances are available to the faint **H α emission** regions, they are all less than 2 kpc (Table 6.3).

With this background, we have made a comparison between Sivan's H maps and our 34.5 MHz maps in the inner Galaxy ($0^\circ < l < 40^\circ$, $|b| < 5^\circ$). We find a good agreement between the bright patches of emission in the **H α** pictures and the 34.5 MHz absorptions. This is shown in Table 6.2 (Y indicates coincidence and N indicates no enhanced **H α emission** - see last column). Wherever we see emission regions in our 34.5 MHz maps there is very little **H α emission**. While there is a practical difficulty

Table 6.3 Coordinates, sizes and distances of the newly discovered regions of H α emission [reproduced from Sivan (1974)]. The equatorial coordinates were computed by us for easy reference to the present survey maps.

No.	Galactic coordinates of the approximate centre		Equatorial coordinates (1950)		Angular size (arc min)	Distance (pc)
	l (d m)	b (d m)	(h m)	(d m)		
1	10	- 2 30	18 14	-21 31	150 x 60	1550
2	117	-11 40	00 12	50 31	330 x 180	1380
3	145	+13 50	04 53	65 25	450 x 240	830
4	161 30	-16	03 50	32 45	540 x 420	-
5	216 30	+ 1	06 59	- 2 39	120 x 60	-
6	218	- 0 30	06 57	- 4 40	90 x 60	-
7	341	- 3 30	17 03	-46 35	90 x 40	-
8	342 30	+ 3	16 40	-41 18	420 x 420	2000
9	351 30	+12	16 35	-28 40	600 x 420	182
10	352	+24	15 58	-20 11	840 x 720	174
11	354	+ 5 30	17 06	-30 48	360 x 60	-

in quantifying the agreement in the positions of the **34.5** MHz absorptions and the **H α emissions** due to the diffuse nature of the latter, the similarity of patterns in the two maps is quite evident. From Table 6.2 it seems reasonable to conclude that almost all of the **HII** regions in our map have optical counterparts. This suggests that these **HII** regions are not too far from the Sun (< 3 kpc).

It is interesting to note that in the longitude range $l = 22^\circ$ to 32° where we see several absorption features there are no optical nebulosities over extended regions (say, 1°) like those commonly found in the longitude range $345^\circ < l < 20^\circ$. On the basis of the discussions in 6.3.1 we think that the absorption features seen in the range $22^\circ < l < 32^\circ$ are also close by (< 6 kpc) and that the poor optical correspondence might be due to severe extinction in this direction. It is interesting to note that the molecular cloud known as 'Acquila Rift' extends from $18^\circ < l < 44^\circ$ and $-6^\circ < b < +10^\circ$ and is 200 pc from us (Dame et al. 1987).

The above conclusion, namely that most of the **HII** regions we see in absorption are within 3 kpc of the sun, can be used to further constrain their linear sizes and electron densities. Most of the **HII** regions seen in our maps will have to be inside the triangle bounded by the line corresponding to 3 kpc distance and the two lines for the two angular diameter limits (Figures 6.5, 6.6 and 6.7). It can be seen from Fig. 6.6 that an electron density of 8 cm^{-3} is consistent with the observed range of $\langle \Delta T \rangle / T_{\text{off}}$ of 0.4 to 0.8 allowing for a range in the distances to the **HII** regions of < 3 kpc. A larger electron density of 16 cm^{-3} (Fig. 6.7) will be consistent only if the **HII** regions are in a

narrow range of distances - between 0.5 kpc and 1 kpc. Given a distance range of < 3 kpc and angular sizes of 0.5° to 2° it follows that most of these **HII** regions have linear sizes of 20 - 80 pc and emission measures from 2000 - 8000 pc cm⁻⁶.

6.3.3 Galactic ridge recombination lines (**GRRL**)

Radio recombination lines of hydrogen from directions in the galactic plane which are free of discrete continuum sources were observed more than 20 years ago by Gottesman and Gordon (1970). Since then a number of observations have been made mainly at centimetre wavelengths (Jackson and Kerr 1971; Gordon and Cato 1972; Mathews, Pedlar and Davies 1973; Jackson and Kerr 1975; **Mebold et al. 1976; Lockman 1976; Hart and Pedlar 1976b**). More recently **recombinaton** line has been observed at metre wavelengths (Anantharamaiah **1985a; 1985b**). There appears to be a consensus that these lines originate from warm ionised gas in weak or evolved **HII** regions or in the outer envelopes of normal **HII** regions (Mathews, Pedler and Davies 1973; Jackson and Kerr 1975; Hart and Pedlar **1975a**; Shaver 1976; **Lockman 1980**). 'Normal' **HII** regions, in the present context, are those thermal sources which can be identified as discrete sources in the continuum surveys of the galactic plane like, for example, the 5 **GHz** survey of Altenhoff et al (1978). Based on the **H272 α** survey (at 325 KHz) of the galactic plane (Anantharamaiah **1985a,b**) and the surveys in **H166 α** (Hart and Pedlar **1976a,b; Lockman 1976**) and **H109 α** (**Downes et al. 1980**), the following five points were made by Anantharamaiah (1986) for the origin of the **GRRLs**:

1) In the first quadrant of the Galaxy, in the longitude range $l < 40^\circ$, the **H272 α** line is detected in every direction observed - 9 against **SNRs**, 6 in blank regions (**i.e.** no normal **HII** region in the observing beam) and 25 against normal **HII** regions. Beyond $l = 40^\circ$, the lines have been detected only towards two strong sources W49 and W51 (there were a total of 8 directions in the range $40^\circ < l < 60^\circ$ centred around $b = 0^\circ$).

2) The gas responsible for the GRRL has electron temperatures of 5000 - 8000 K, emission measures of 3000 pc cm^{-6} and path lengths of 50 - 200 pc.

3) There is a general agreement between the longitude-velocity diagrams constructed with **H272 α** , **H166 α** and **H109 α** lines.

4) The high emission measure ($10^4 - 10^5 \text{ pc cm}^{-6}$), small diameter (few arc min) **H109 α** sources cannot produce any appreciable **H272 α** emission due to the large optical depth, pressure broadening and beam dilution effects at 325 MHz (the beam size was $6 \times 2^\circ$ in the observations by Anantharamaiah 1985a,b)

5) Most of the GRRLs arise in low density envelopes of conventional **HII** regions, whose compact cores give rise to **H109 α** .

6.3.4 Discrete absorptions seen at 34.5 MHz and their relation to GRRLs

In this section we would like to explore a different viewpoint viz., how much of the GRRLs can be accounted for by the discrete absorptions that we have observed. **We would** like to

relate our observations to the **H272 α** , **H166 α** and **H109 α** observations of the galactic plane.

The following common points between 34.5 MHz absorptions and the GRRLs are worth noting:

1) In the first quadrant of the Galaxy both the absorptions and the GRRLs are seen only in the range of $0^\circ < l < 40^\circ$.

2) For an assumed electron temperature of 8000 K, the emission measures and the sizes of the **HII** regions as implied by the 34.5 MHz absorptions are similar to those derived from the GRRLs.

3) There is a qualitative agreement between the intensity of the **H166 α** line as a function of the Galactic longitude and the presence or absence of deep absorptions seen at 34.5 MHz. : The **H166** surveys done by **Lockman** (1976) and Hart and Pedlar (1976b) have half power beamwidths of $21'$ and $31' \times 33'$ respectively. This is very close to the resolution of the present survey. A look at figure 6.8 shows maxima in the intensity of the **H166 α** line at longitudes of 7° , 14° , 25° , 31° , 38° and minima at longitudes of 20° and 36° . As can be seen from our maps, these positions correspond to deep and shallow absorptions.

Both at $l = 358^\circ$ and $l = 2^\circ$ there is very little **H166 α** emission (**Lockman** 1976). These two regions are seen in emission on the 34.5 MHz map separated by a deep absorption at $l = 0^\circ$ where strong **H166 α** emission is seen.

4) Most of the directions in which the **H 272 α lines** have been detected also coincide with the direction of one or more of the discrete absorptions seen at 34.5 MHz.

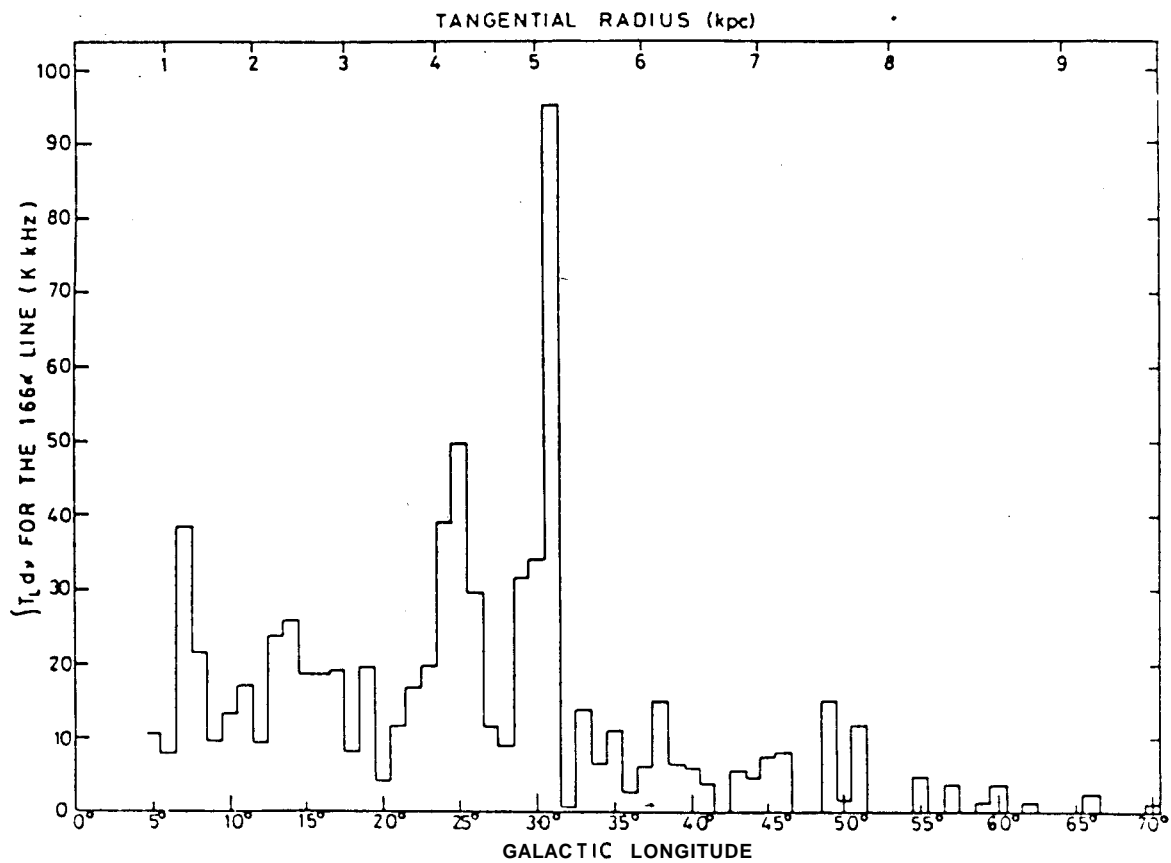


Fig. 6.8: The intensity of the H166 α line, $\int T_L d\gamma$, as a function of galactic longitude derived from spectra separated by 1° along the galactic plane (reproduced from Hart and Pedlar (1976b)).

Based on these points we wish to suggest that most of the GRRLs originate in the ionised gas that is seen in absorption at 34.5 MHz. Since the considerations outlined before suggest that the gas responsible for the absorption at 34.5 MHz is nearby (≈ 3 kpc), this implies that most of the GRRLs also originate in this nearby gas.

But do all the GRRLs originate in the nearby HII regions? It does not appear so. A close look at the l - V diagram (Fig. 6.9) reveals that except for the 100 km s^{-1} feature in the longitude range of 25° to 35° , most others are $\lesssim 50 \text{ km s}^{-1}$. The Schmidt model of galactic rotation implies a 'near' distance of $\lesssim 4$ kpc for the lower velocity branch of the l - V diagram. Thus most of the lower velocity branch can be explained by the absorptions seen in the present survey. But the higher velocity gas has to have a different explanation.

Gas at 100 km s^{-1} has been seen in the longitude range $22^\circ < l < 32^\circ$ in the $\text{H}109\alpha$, $\text{H}166\alpha$ and $\text{H}272\alpha$ line observations. The Schmidt model of galactic rotation puts this gas at around 8 kpc from us. In these longitude ranges one is looking along the length of the Scutum arm and picking up several discrete HII regions and diffuse gas in the spiral arm present along the line of sight. Due to its distance we don't expect to see this gas in absorption in the low frequency observation.

6.3.5 What are the discrete absorptions ?

We would like to briefly discuss here the discrete absorptions that we see at 34.5 MHz in relation to the compact HII regions of the kind **found** in the high frequency continuum

surveys like for example the 5 GHz survey by Altenhoff et al. (1978). This survey covered the Galactic longitude range of $0^\circ < l < 60^\circ$ and $|b| < 0.5^\circ$. Most of the HII regions identified in this survey are compact with angular sizes of $\approx 5'$. These compact HII regions can not produce any significant absorption on our 34.5 MHz maps due to the large beam dilution they suffer.

If all of these compact HII regions have envelopes around them as has been postulated by Lockman (1980) and Anantharamaiah (1986) then such extended HII regions may not suffer from beam dilution in our observations. Further, they would produce absorptions at 34.5 MHz provided there is not too much foreground emission, i.e. if they are sufficiently near by. Let us see whether there is any observational evidence to this.

Recently Lockman (1989) has made an extensive survey of radio recombination lines from nearly 500 continuum sources in the longitude range $350^\circ < l < 250^\circ$. He was able to detect the H85 α , H87 α and H88 α recombination lines from 462 sources.

(a) 390 of these sources are in the longitude range 0° to 90° . Most of these are in the latitude range $|b| \lesssim 1^\circ$. Let us assume that these compact HII regions have extended envelopes around them ($\approx 50 - 200$ pc) as has been postulated in the literature. As was argued above one would expect the near by ones ($\lesssim 3$ kpc) to produce significant absorption. Unfortunately, there are no reliable distance estimates to these HII regions; because of the distance ambiguity in this quadrant there is an estimate of the 'near' distance and the 'far' distance. If most of these HII regions are at the 'far' distance (i.e. ≈ 11 to 15 kpc) then one

would not expect to see them in absorption. However, this is unreasonable because in this case many of these **HII** regions would have to be ≈ 250 pc from the plane. Hence, at least some of these sources have to be at their 'near' distance (≈ 3 kpc), and hence produce discrete absorption features. However, as can be seen from our maps there is very little absorption beyond $l = 32^\circ$ (in this quadrant). Hence it is difficult to reconcile with the picture in which all of the sources have extended envelopes.

(b) Let us continue with the comparison with Lockman's observations (1989) beyond $l = 90^\circ$. Unfortunately, in the range $l = 90^\circ$ to 150° meaningful comparison is made difficult due to the residual sidelobes of Cas A. Beyond this region ($150^\circ < l < 250^\circ$) and $|b| < 10^\circ$ Lockman (1989) has detected **H87 α** line from 18 sources. Of these, only 3 are in the directions where we see absorption. That still leaves 15 directions in which we do not see absorptions. This could in principle be reconciled if all of these are well beyond 3 kpc. Even if one grants this there is an additional difficulty. In this longitude range there are 6 discrete absorption features in the 34.5 MHz map and there are no **H87 α** sources in these directions.

We have just seen that there are directions in which both **H87 α** line emitting gas and discrete absorptions at low frequencies are seen. If one accepts the hypothesis that these absorption features are in fact produced by the envelopes of compact **HII** regions then one can get limits on the sizes of these envelopes. Most of these discrete absorption features are $\approx 1^\circ$. Since the gas producing this absorption will have to be located within ≈ 3 kpc it **follows** that if this gas has to be associated

with the envelopes of **HII** regions then these envelopes can not be much bigger than 50 pc. However, as was mentioned before the model in which the **H166 α** and the **H272 α** line emitting gas is identified with the envelopes, the linear sizes of these envelopes have to be in the range of 50 - 300 pc (**Lockman** 1980; **Anantharamaiah** 1986). Even a conservative size of ≈ 150 pc for the envelope will imply an angular size of $\approx 3^\circ$ for the absorption features. Such extended absorption features are not present in our maps.

Faced with these difficulties, we have looked for an alternative picture to account for the discrete absorptions seen by us. We feel that these may be due to old and evolved **HII** regions and may not be related to the general population of compact **HII** regions. At first sight this might be in conflict with the apparent agreement between the velocities of **H109 α** , **H166 α** and **H272 α** lines (Fig. 6.9). In our opinion this may not be a serious problem. As has been pointed out by **Lockman** (1976) and **Anantharamaiah** (1985a), the **H166 α** and **H272 α** lines are broad, weak and may have multiple velocity components. Thus, it is not at all clear how much of **H166 α** and **H272 α** line source is associated with the **H109 α** line source. It is conceivable that a nearby, diffuse gas can give rise to **H166 α** and **H272 α** lines while not contributing to **H109 α** line.

6.3.6 Conclusions

1. Discrete absorptions seen at 34.5 MHz must be due to nearby (< 3 kpc), extended (20 - 100 pc) and **low** density (10 cm^{-3}) **HII** regions. It should be noted that even the upper limit to the

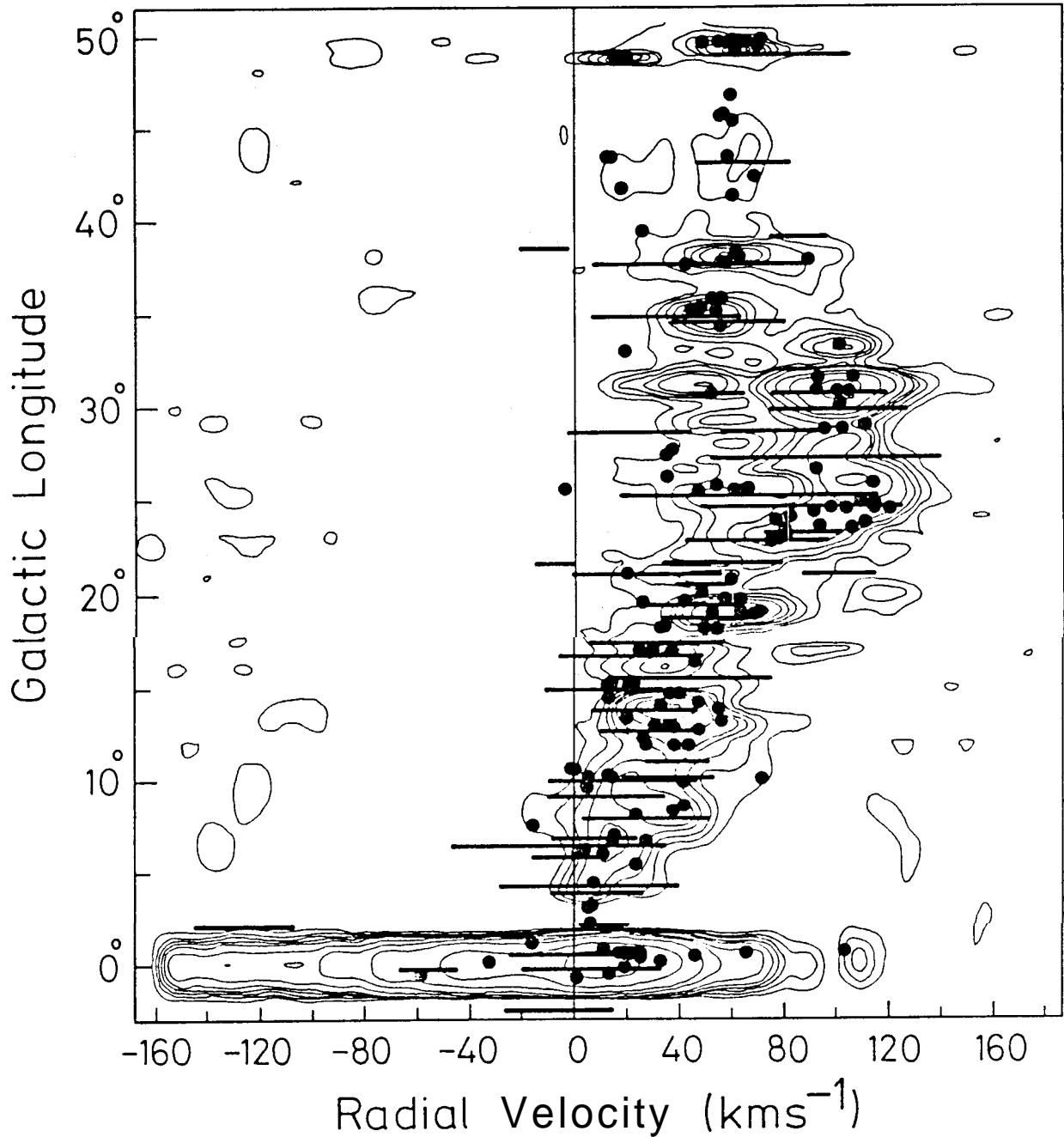


Fig. 6.9: Longitude - velocity diagram of the recombination lines H272 α (horizontal lines), H166 α (contours) and H110 α (dots). The horizontal lines indicate the observed half-power width of the H272 α lines. The data for the three lines are taken from Anantharamaiah (1985a), Lockman (1976) and Downes et al. (1980) respectively. This figure is reproduced from Anantharamaiah (1986).

linear sizes of these regions is less than that proposed by Anantharamaiah (1986).

2. The low velocity ($\lesssim 50 \text{ km s}^{-1}$) $\text{H166}\alpha$ and $\text{H272}\alpha$ recombination lines can easily be accounted for by such **HII** regions.

3. Our interpretation of the discrete absorptions observed at 34.5 MHz has thrown considerable doubt on the core-envelope picture of the **HII** regions at least as applied to the origin of the GRRLs. In our opinion the GRRLs may originate in old, evolved **HII** regions.

REFERENCES

- Altenhoff, W.J., **Mezger**, P.G., Strassl, H., Wendker, H., Westerhout, G. 1960, Veroff Sternwarte, **Bonn59**, 48.
- Altenhoff, W.J., Downes, D., Pauls, T., Schraml, J. 1978, Astr. Astrophys. Suppl. Ser., **35**, 23.
- Anantharamaiah, K.R. **1985a**, J. Astrophys. Astr., 6, 177.
- Anantharamaiah, K.R. **1985b**, J. Astrophys. Astr., 6, 203.
- Anantharamaiah, K.R. 1986, J. Astrophys. Astr., 7, 131.
- Dame, T.M., Ungerechts, H., Cohen, R.S., de Geus, E.J., Gremer, I.A., May, J., Murphy, D.C., Nyman, L.A., Thaddeus, P. 1987, Astrophys. J., 322, 706.
- Downes, D., Wilson, T.L., Bieging, J., Wink, J. 1980, Astr. Astrophys. Suppl. Ser., 40, 379.
- Georgelin, Y.P., Georgelin, Y.M. 1970, Astr. Astrophys., **6**, 349.
- Gordon, M.A., Cato, T. 1972, Astrophys. J., 176, 587.
- Gottesman, S.T., Gordon, M.A. 1970, Astrophys. J., 162, L93.
- Hart, L., Pedlar, A. **1976a**, Mon. Not. R. astr. **Soc.**, 176, 135.
- Hart, L., Pedlar, A. **1976b**, Mon. Not. R. astr. **Soc.**, 176, 547.
- Haslam**, C.G.T., Salter, C.J., **Stoffel**, H., Wilson, W.E. 1982, Astr. Astrophys. Suppl., 47, 1.
- Jackson, P.D., Kerr, F.J. 1971, Astrophys. J., 168, 29.
- Jackson, P.D., Kerr, F.J. 1975, Astrophys. J., 196, 723.
- Kerr, F.J. 1957, Astr. **J.**, **62**, **93**.
- Lockman**, F.J. 1976, Astrophys. J., 204, 429.
- Lockman**, F.J. 1980, in 'Radio Recombination Lines', Ed. **P.A.** Shaver, D. **Reidel**, Dordrecht, p. 185.
- Lockman**, F.J. 1989, preprint.
- Mathews, H.E., Pedlar, A., Davies, R.D. 1973, Mon. Not. R. astr. **Soc.**, 165, 149.
- Mebold**, U., Altenhoff, W.J., Churchwell, E., Walmsley, C.M., 1976, Astr. Astrophys., 53, 175.
- Reich, P., Reich, W. 1988, Astr. Astrophys. **Suppl. Ser.**, 74, 7.

Rodgers, A.W., Campbell, C.T., Whiteoak, J.B. 1960,
Mon. Not. R. astr. Soc., 121, 103.

Sancisi, R. 1976, Astr. Astrophys., 53, 159.

Shaver, P.A. 1976, Astr. Astrophys. 49, 1.

Sivan, J.P. 1974, Astr. Astrophys. Suppl. Ser., 16, 163.

BIBLIOGRAPHY

- Abramowitz, M., Stegun, I.A. , Eds. Handbook of Mathematical Functions, New York, Dover Publications Inc.
- Abranin, E.P., Bazelyan, L.L., Goncharov, N.Yu. 1977,**
Sov. Astr., 21, 441.
- Altenhoff, W.J., Mezger, P.G., Strassl, H., Wendker, H.,
Westerhout, G. 1960, Veroff Sternwarte, **Bonn59**, 48.
- Altenhoff, W.J., Downes, D., Pauls, T., Schraml, J. 1978,**
Astr. Astrophys. Suppl. Ser., **35**, 23.
- Anantharamaiah, K.R. **1985a**, J. Astrophys. Astr., 6, 177.
- Anantharamaiah, K.R. **1985b**, J. Astrophys. Astr., 6, 203.
- Anantharamaiah, K.R. 1986, J. Astrophys. Astr., 7, 131.
- Baars, J.W.M., Genzel, R., Pauliny-Toth, I.I.K., Witzel, A. 1977,
Astr. Astrophys., **61**, 99.
- Ballarati, B., Feretti, L., Ficarra, A., Gavazzi, G., Giovannini, G.,
Nanni, M., Olori, M.C. 1981, Astr. Astrophys., 100, 323.**
- Beichman, C.A. 1987, Ann. Rev. Astr. Astrophys., 25, 521.
- Berkhuijsen, E.M. 1971, Astr. Astrophys., 14, 359.**
- Berkhuijsen, E.M., Haslam, C.G.T., Salter, C.J. 1971,**
Astr. Astrophys., **14**, 252.
- Bhattacharya, D., **Srinivasan, G. 1986, Curr. Sci., 55, 327.**
- Bowers, F.K., Klinger, R.S. 1974,
Astr. Astrophys. Suppl. **Ser., 15, 373.**
- Braude, **S.Ya., Lebedeva, O.M., Megn, A.V., Ryabov, B.P.,
Zhouk, I.N. 1969, Mon. Not. R. astr. Soc., 143, 289.**
- Bridle, A.H., Purton, C.R. 1968, Astr. J., 73, 717.
- Caswell, J.L. **1976, Mon. Not. R. astr. Soc., 177, 601.**
- Caswell, J.L., Lerche, I. 1979, Mon. Not. R. astr. Soc., 187, 201.**
- Christiansen, W.N., Hogbom, J.A. 1985, Radiotelescopes,
Cambridge University Press.
- Clark, D.H., Caswell, J.L. 1976, Mon. Not. R. astr. Soc., 174, 267.**

- Dame, T.M., Ungerechts, H., Cohen, R.S., de Geus, E.J., Gremer, I.A., May, J., Murphy, D.C., **Nyman**, L.A., Thaddeus, P. 1987, *Astrophys. J.*, 322, 706.
- Deshpande, A.A., Shevgaonkar, R.K., Sastry, Ch.V.** 1984, *Astrophys. Space Sci.*, 102, 21.
- Deshpande, A.A., Sastry, Ch.V.** 1986, *Astr. Astrophys.*, **160**, 129.
- Deshpande, A.A. 1987, **Ph.D.** Thesis, Dept. of El. Eng., Indian Institute of Technology, Bombay.
- Downes, D., Wilson, T.L., Bieging, J., Wink, J. 1980, *Astr. Astrophys. Suppl. Ser.*, 40, 379.
- Duin, R.M., van der Laan, H.** 1975, *Astr. Astrophys.*, 40, 111.
- Dwarakanath, K.S., Shevgaonkar, R.K., Sastry, Ch.V.** 1982, *J. Astrophys. Astr.*, **3**, 207.
- Erickson, W.C. 1983, *Astrophys. J.*, 264, L13.
- Georgelin, Y.P., Georgelin, Y.M. 1970, *Astr. Astrophys.*, **6**, 349.
- Gordon, M.A., Cato, T. 1972, *Astrophys. J.*, 176, 587.
- Gottesman, S.T., Gordon, M.A.** 1970, *Astrophys. J.*, **162**, L93.
- Graham, D.A., Haslam, C.G.T., Salter, C.J., Wilson, W.E.** 1982, *Astr. Astrophys.* 109, 145.
- Green, D.A. 1988, *Astrophys. Space Sci.*, 148, 3.
- Hanisch, R.J.** 1980, *Astr. J.*, 85, 1565.
- Hart, L., Pedlar, A. **1976a**, *Mon. Not. R. astr. Soc.*, 176, 135.
- Hart, L., Pedlar, A. **1976b**, *Mon. Not. R. astr. Soc.*, 176, 547.
- Haslam, C.G.T., Salter, C.J., Stoffel, H., Wilson, W.E.** 1982, *Astr. Astrophys. Suppl. Ser.*, 47, 1.
- Hester, J.J., Parker, R.A.R., Dufour, R.J. 1983, *Astrophys. J.*, 273, 219.
- Hogbom, J. 1974, *Astrophys. J. Suppl.* **15**, 417.
- Jackson, P.D., Kerr, F.J. 1971, *Astrophys. J.*, **168**, 29.
- Jackson, P.D., Kerr, F.J. 1975, *Astrophys. J.*, 196, 723.
- Jaffe, W.J., Rudnick, L.** 1979, *Astrophys. J.*, 233, 453.
- Jansky, K.G. 1932, *Proc. IRE*, 20, 1920.

- Jones, B.B., **Finlay**, E.A. 1974, *Aust. J. Phys.*, **27**, 687.
- Kassim, N.E. 1988, *Astrophys. J. Suppl. Ser.*, 68, 715.
- Kellermann, K.I., Pauliny-Toth, I.I.K., Williams, P.J.S. 1969,
Astrophys. J., 157, 1.
- Kenderdine**, S. 1963, *Mon. Not. R. astr. Soc.*, **126**, 55.
- Kerr, F.J. 1957, *Astr. J.*, **62**, 93.
- Kulkarni, S.R., Narayan, R. 1988, *Astrophys. J.*, **335**, 755.
- Kundu**, M.R., **Velusamy**, T. 1967, *Ann. d'Astrophysique*, **30**, 723.
- Large**, M.I., **Quigley**, M.J.S., **Haslam**, C.G.T. 1962,
Mon. Not. R. Astr. Soc., 124, 405.
- Lockman**, F.J. 1976, *Astrophys. J.*, 204, 429.
- Lockman**, F.J. 1980, in 'Radio Recombination Lines',
Ed. **P.A. Shaver**, **D. Reidel**, Dordrecht, p. 185.
- Lockman**, F.J. 1989, preprint.
- Mahoney**, M.J., Erickson, W.C. 1985, *Nature*, **317**, 154.
- Mathews, H.E., Pedlar, A., Davies, R.D. 1973,
Mon. Not. R. astr. Soc., 165, 149.
- Mathewson**, D.S., **Healey**, J.R., **Rome**, J.M. 1962,
Aust. J. Phys., **15**, 354.
- Mathewson, D.S., Broten, N.W., Cole, D.J. 1965,
Aust. J. Phys., **18**, 665.
- Mebold**, U., Altenhoff, W.J., Churchwell, E., Walmsley, C.M.,
1976, *Astr. Astrophys.*, **53**, 175.
- Milne**, D.K. 1968, *Aust. J. Phys.*, 21, 201.
- Milne**, D.K. 1980, *Astr. Astrophys.*, 81, 293.
- Milne**, D.K., **Manchester**, R.N. 1986, *Astr. Astrophys.*, 167, 117.
- Milogradov-Turin**, J., **Smith**, F.G. 1973, *Mon. Not. R. Astr. Soc.*,
161, 269.
- Odegard**, N. 1986, *Astrophys. J.*, 301, 813.
- Parkes**, G.E., **Charles**, P.A., **Culhane**, J.L., **Ives**, J.C. 1977,
Mon. Not. R. astr. Soc., 179, 55.
- Quigley**, M.J.S., **Haslam**, C.G.T. 1965, *Nature*, 208, 741.

- Radhakrishnan, V., Brooks, J.W., Goss, W.M., Murray, **J.D.**,
Schwarz, U.J. 1972, *Astrophys. J. Suppl. Ser.*, **24**, 1.
- Rappaport, S., **Pétre**, R., Kayat, M.A., Evans, K.D.,
Smith, G.C., **Levine**, A. 1979, *Astrophys. J.*, 227, 285.
- Ravindra, D.K. 1983, **Ph.D.** Thesis, Dept. of El. Com. Eng.,
Indian Institute of Science, Bangalore.
- Read, R.B., 1963, *Astrophys. J.*, **138**, 1.
- Reber, G. 1940, *Astrophys. J.*, 91, 621.
- Reich, P., Reich, W. 1988, *Astr. Astrophys. Suppl. Ser.*, **74**, 7.
- Rishbeth**, H. 1958, *Aust. J. Phys.*, 11, 550.
- Rodgers, A.W., Campbell, C.T., Whiteoak, J.B. 1960,
Mon. Not. R. astr. Soc., 121, 103.
- Roger, R.S., **Costain**, C.H., Lacey, J.D. 1969, *Astr. J.*, **74**, 366.
- Sancisi, R. 1976, *Astr. Astrophys.*, **53**, 159.
- Sastry**, Ch.V., **Dwarakanath**, K.S., **Shevgaonkar**, R.K. 1981,
J. Astrophys. Astr., 2, 339.
- Sastry**, Ch.V., **Shevgaonkar**, R.K. 1983, *J. Astrophys. Astr.*, 4, 47.
- Shain, C.A., Komesaroff, M.M., Higgins, C.S. 1961,
Aust. J. Phys., **14**, 508.
- Shaver**, P.A. 1969, *Mon. Not. R. astr. Soc.*, 142, 273.
- Shaver**, P.A., **Goss**, W.M. 1970, *Aust. J. Phys. Suppl.*, **14**, 77.
- Shaver, P.A. 1976, *Astr. Astrophys.* **49**, 1.
- Shaver, P.A., Pierre, M. 1989, ESO preprint, No. 637.
- Sivan, J.P. 1974, *Astr. Astrophys. Suppl. Ser.*, **16**, 163.
- Sofue**, Y., **Reich**, W., **Reich**, P. 1988, NRO preprint no. 196.
- Swarup, G., Sarma, N.V.G., Joshi, M.N., Kapahi, V.K.,
Bagri, D.S., Damle, S.H., Ananthakrishnan, S.,
Balasubramanian, V., Bhave, S.S., **Sinha**, R.P. 1971,
Nature, 230, 185.
- Terzian**, Y., **Balick**, B. 1969, *Astr. J.*, 74, 76.
- Tuohy**, I.R., **Clark**, D.H., **Garmine**, G.P., 1979,
Mon. Not. R. astr. Soc., 189, **59p**.

- Udayashankar, N. 1986, **Ph.D.** Thesis, Dept. of Physics,
Bangalore University, Bangalore.
- van Vleck, J.H., Middleton, D. 1966, Proc. IEEE, 54, 2.
- Viner, M.R., Erickson, W.C. 1975, Astr. J., 80, 931.
- Wakker, B.P.**, Schwarz, U.J. 1988, Astr. Astrophys., 200, 312.
- Weiler, K.W.**, Panagia, N. 1980, Astr. Astrophys., 90, 269.
- Weiler, K.W.** 1983, Supernova Remnants and their X-ray Emission,
p.299 - 320, Eds. **J.Danziger** and **P.Gorenstein**.
- Williams, P.J.S., Kenderdine, S., **Baldwin**, J.E. 1966,
Mem. R. astr. **Soc.**, 70, 53.
- Willson, M.A.G.** 1970, Mon. Not. R. astr. **Soc.**, 151, 1.